Article

Pyrazole-4-Carboxamide (YW2065): A Therapeutic Candidate for Colorectal Cancer via Dual Activities of Wnt/#-Catenin Signaling Inhibition and AMP-Activated Protein Kinase (AMPK) Activation

Wei Yang, yingjun li, Yong Ai, Obinna N. Obianom, Dong Guo, Hong Yang, Srilatha Sakamuru, Menghang Xia, Yan Shu, and Fengtian Xue

J. Med. Chem., **Just Accepted Manuscript** • DOI: 10.1021/acs.jmedchem.9b01252 • Publication Date (Web): 26 Nov 2019

Pyrazole-4-Carboxamide (YW2065): A Therapeutic Candidate for Colorectal Cancer via Dual Activities of Wnt/*β*-Catenin Signaling Inhibition and AMP-Activated Protein Kinase (AMPK) Activation

Wei Yang,[#,1,⊥] Yingjun Li,[#,1] Yong Ai,[1] Obinna N Obianom,[1] Dong Guo,[1] Hong Yang,[1] Srilatha Sakamuru,[2] Menghang Xia,[2] Yan Shu,*[,1,3] and Fengtian Xue*[,1]

[1]Department of Pharmaceutical Sciences, University of Maryland School of Pharmacy, Baltimore, Maryland 21201, United States

[2]9800 Medical Center Drive, National Center for Advancing Translational Sciences, National Institutes of Health, Bethesda, Maryland 20892, United States

[3]School and Hospital of Stomatology, Guangzhou Medical University, Guangzhou 510140, China

[#]These authors contributed equally to this work.

Corresponding Authors

*Y.S.: phone, 410-706-7493; fax, 410-706-0886; e-mail, yshu@rx.umaryland.edu

*F.X.: phone, 410-706-8512; fax, 410-706-0886; e-mail, fxue@ rx.umaryland.edu

ABSTRACT

Dysregulation of the Wnt/β-catenin signaling pathway has been widely recognized as a pathogenic mechanism for colorectal cancer (CRC). Although numerous Wnt inhibitors have been developed, they commonly suffer from toxicity and unintended effects. Moreover, concerns have been raised in targeting this pathway because of its critical roles in maintaining stem cells and regenerating tissues and organs. Based on the anthelmintic drug pyrvinium and previous lead FX1128, we have developed a compound YW2065 (**1c**), which demonstrated excellent anti-CRC effects *in vitro* and *in vivo*. YW2065 achieves its inhibitory activity for Wnt signaling by stabilizing Axin-1, a scaffolding protein that regulates proteasome degradation of β-catenin. Simultaneously, YW2065 also led to the activation of the tumor suppressor AMPK, providing an additional anti-cancer mechanism. In addition, YW2065 showed favorable pharmacokinetic properties without obvious toxicity. The anti-CRC effect of YW2065 was highlighted by its promising efficacy in a mice xenograft model.

INTRODUCTION

Colorectal cancer (CRC) is the third most frequently occurring cancer and the second leading cause of cancer-related death in the United States.[1,2] Although patients with early-stage CRC can be treated with surgical resection followed by adjuvant therapy, approximately 50% of CRC patients will develop metastases, which require systemic medical treatment and lead to high mortality rates.[3] Available drugs for metastatic CRC (mCRC) are limited to chemotherapies such as the thymidylate synthase inhibitors (e.g., 5-FU and folinic acid) and DNA-alkylating agents (e.g., oxaliplatin and irinotecan). Recently, biologics targeting the vascular endothelial growth factor (VEGF; bevacizumab) and epidermal growth factor receptor (EGFR; cetuximab and panitumumab) started to emerge,[4-6] however, they fail to improve patients' survival rate significantly.[2] Thus, novel therapeutics for the treatment of mCRC is still urgently needed.

Over 90% of mCRC patients carry genetic mutations associated with upregulated Wnt signaling,[7] which makes this pathway an attractive target against mCRC.[8] The Wnt/β-catenin signaling pathway regulates the expression of its target genes through the Wnt ligands and intracellular signal transducer β-catenin (Figure 1). During the "off state" of the pathway when Wnt proteins are not interacting with the LRP6 and Fz receptors, a cytoplasmic "destruction complex" is formed by the scaffolding protein Axin and adenomatous polyposis coli (APC). This complex facilitates the phosphorylation of β-catenin by casein kinase 1α (CK1α) and glycogen synthase kinase 3β (GSK3β), leading to the proteasomal degradation of β-catenin. During the "on-state", the formation of the destruction complex is prohibited. As a result, β-catenin is accumulated and translocated

into the nucleus, where it binds to the transcriptional factor LEF/TCF along with other transcriptional coactivators (CBP, P300, PYGO and BCL9), and activates the expression of its target genes to promote cell proliferation, differentiation and growth.

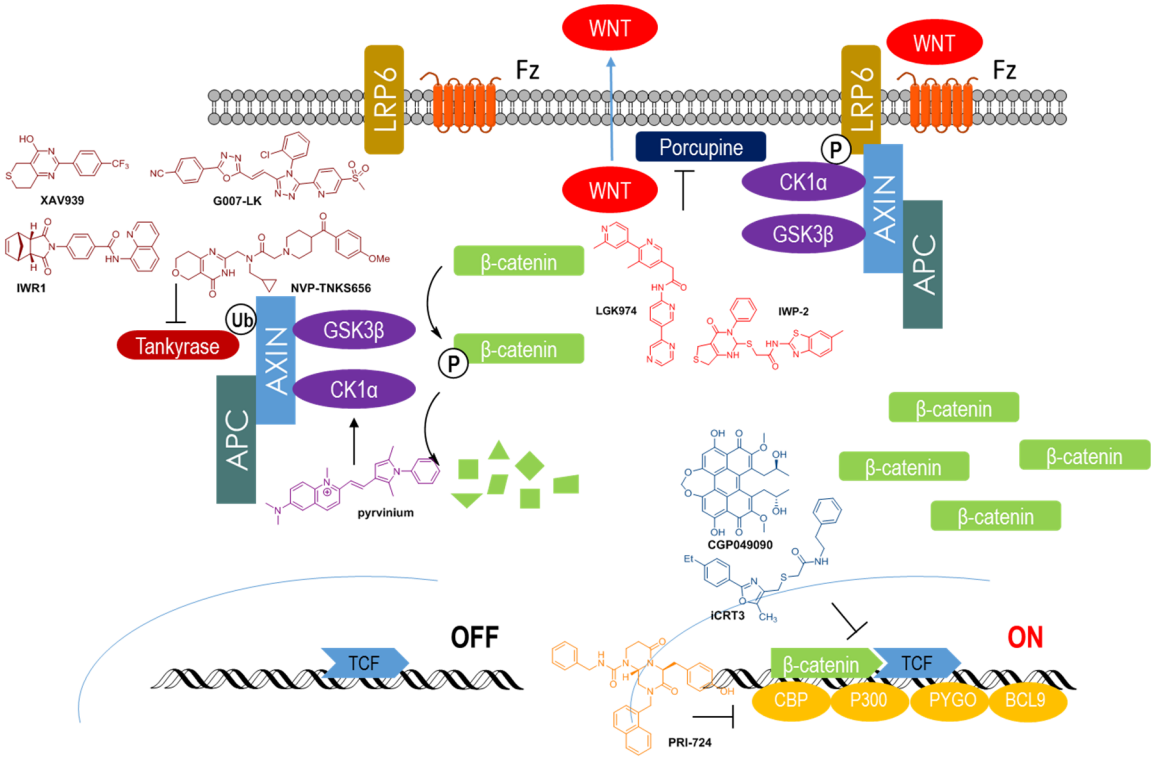

Figure 1. The Wnt/*β*-catenin signaling pathway and examples of known inhibitors.

Several classes of Wnt inhibitors are known by targeting different components of the pathway (Figure 1).[9-13] The Novartis clinical candidate LGK974[14] and its analogs[15,16] (e.g., IWP-2) are porcupine inhibitors, which function by blocking the secretion of the Wnt ligands. In addition, inhibitors have been developed to target key protein-protein interactions (PPI) involving *β*-catenin in the nucleus. For example, CGP049090[17] and iCRT3 analogs[18] inhibit the PPI between *β*-catenin and LEF/TCF, while the Prism/Eisai pharmaceuticals clinical candidate PRI-724 selectively blocks the PPI of *β*-catenin with CBP.[19] Although targeting the downstream PPIs demonstrated unique specificities, these

compounds have suffered from varying degrees of toxicity and unintended effects on tissue homeostasis. Moreover, XAV939,[20] IWR-1,[16] G007-LK,[21] and NVP-TNKS656[22] are inhibitors of tankyrase (TNKS), a member of poly(ADP-ribose) polymerases (PARPs). However, competitive inhibitors of TNKS turned out to be insufficient because polymerization of TNKS, *via* SAM domains, promotes Wnt signaling independently of the catalytic activity.[23] In addition, TNKS recruits and PARylates numerous protein partners[24-26] *via* an ankyrin (ANK)-repeat domain, for various biological purposes, therefore, targeting the active site may also lead to potential toxicities.[27,28] Finally, the anthelmintic drug pyrvinium has been reported as a Wnt inhibitor by activating CK1α.[29] However, pyrvinium has extremely low oral bioavailability and high toxicity, which prohibits its further application as an anti-cancer therapeutic agent.[30] Using pyrvinium as a template, our laboratory recently developed a compound FX1128 (Figure 2), which demonstrated excellent inhibitory potency for Wnt signaling, although the anti-proliferation efficacy of FX1128 was limited (Figure S1).[31]

In addition to genetic alteration, reprogramming of cellular metabolic pathways is also commonly associated with mCRC.[32,33] The adenosine monophosphate (AMP)-activated protein kinase (AMPK), as a metabolic switch, plays a crucial role in metabolic disorders and carcinogenesis in the intestine.[34] Activated AMPK phosphorylates the serine and threonine residues on its substrates, resulting in energy restoration and tumor suppression.[35] For instance, AMPK activation was reported to be a prognostic factor for mCRC patients receiving chemotherapy in combination with the VEGF-targeting monoclonal antibody drug bevacizumab.[36] It was also known that AMPK activators, such as metformin and aspirin, induced anti-proliferative cytotoxicity against CRC cells.[37-40]

The complexity of mCRC usually requires combination therapies that attack multiple anticancer machineries. Therefore, drugs that target dual or multiple pathways often result in improved anticancer efficacy and delayed drug resistance.[40,41] We hypothesized that compounds that simultaneously inhibit Wnt signaling and activate AMPK pathway can be promising therapeutics for the treatment of mCRC. [41,42]

Herein, we report the synthesis and characterization of a new series of anti-mCRC compounds (**1a-s** and **2a-e**) with dual activities of Wnt inhibition and AMPK activation (Figure 2). The chemical structures of new inhibitors were based on our previous lead FX1128 by replacing its triazole core, which caused weak anti-cancer activity and poor aqueous solubility, with a pyrazole ring, a widely used drug-like group in small molecule drug design. One new compound of the series, YW2065, not only maintained excellent inhibitory potency for the Wnt signaling, but also potently activated the AMPK pathway. The dual functional compound YW2065 demonstrated promising anti-mCRC effects *in vitro* and *in vivo*.

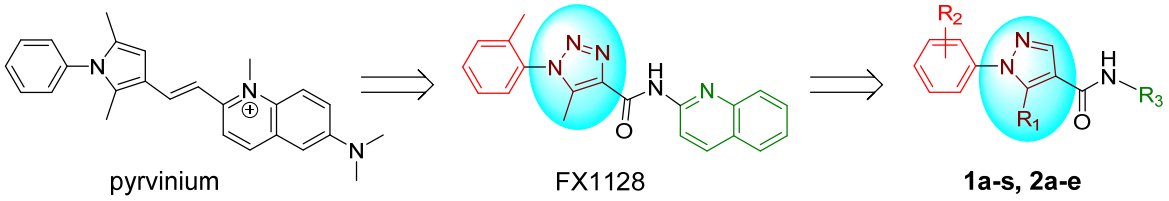

Figure 2. The design strategy of pyrazole-based compounds **1a-s** and **2a-e**.

RESULTS AND DISCUSSION

Synthesis. The syntheses of compounds **1a-s** are detailed in Scheme 1. Condensation of ethyl acetoacetate (**3**) with *N*,*N*-dimethylformamide dimethyl acetal in EtOH provided compound **4** in good yields. Next, pyrazole formation using compound **4** and a substituted hydrazine in the presence of DIPEA led to the generation of the ester intermediate, which was submitted to a hydrolysis using aqueous NaOH to afford carboxylic acids **5a-p** in good yields. Finally, PyCIU-mediated coupling of acids **5a-p** with various aromatic amines yielded the final products **1a-s** in moderate to good yields.

Scheme 1. Synthesis of compounds **1a-s**[a]

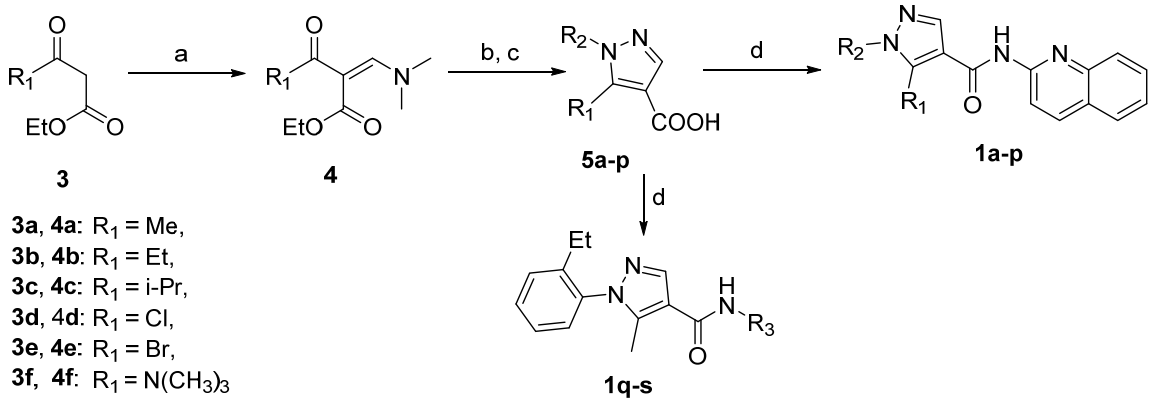

5,1a: R_1 = Me, R_2 = Ph
5,1b: R_1 = Me, R_2 = 2-F-Ph
5,1c: R_1 = Me, R_2 = 2-Br-Ph
5,1d: R_1 = Me, R_2 = 2-Et-Ph
5,1e: R_1 = Me, R_2 = 2,6-diF-Ph
5,1f: R_1 = Me, R_2 = 2-F-6-Br-Ph
5,1g: R_1 = Me, R_2 = 2,4-diF-Ph
5,1h: R_1 = Me, R_2 = 2-F-3-Cl-Ph
5,1i: R_1 = Me, R_2 = 2,5-diMe-Ph
5,1j: R_1 = Me, R_2 = 2,6-diMe-Ph
5,1k: R_1 = Me, R_2 = 3-Me-Py
5,1l: R_1 = Cl, R_2 = Ph
5,1m: R_1 = Br, R_2 = Ph
5,1n: R_1 = Et, R_2 = Ph
5,1o: R_1 = *i*-Pr, R_2 = Ph
5,1p: R_1 = $N(CH_3)_3$, R_2 = Ph
1q: R_3 = 2-naphthalene
1r: R_3 = 3-isoquinoline
1s: R_3 = 2-6-methylpyridine

[a]Reagents and conditions: (a) DMF-DMA, EtOH, 60 °C, 97%; (b) R_3-$NHNH_2$, DIPEA, EtOH, 60 °C; (c) NaOH, EtOH/H_2O, reflux, 40-98% for two steps; (d) aromatic amines, PyCIU, DIPEA, DCE, 80 °C, 24-88%.

The synthesis of compounds **2a-e** began with anilines **6a-c** (Scheme 2). Diazotization of the amino group of compounds **6a-c** using $NaNO_2$ in HCl (aq.), followed by condensation of the diazotized anilines with ethyl 2-chloro-3-oxobutanoate in the presence of NaOAc yielded hydrazonoyl chlorides **7a-c**. Next, reaction of compounds **7a-c** with either diethyl (2-oxopropyl) phosphonate, 4-(cyclopent-1-en-1-yl)morpholine, or 4-(cyclohex-1-en-1-yl)morpholine triggered a cyclization reaction to give the ethyl esters. Then, saponification of the ethyl esters in aqueous NaOH provided pyrazole-3-carboxylic acids **8a-e** in good yields. Finally, the PyCIU-mediated coupling of acids **8a-e** with 2-aminoquinoline yielded compounds **2a-e** in moderate to good yields.

Scheme 2. Synthesis of compounds **2a-e**[a]

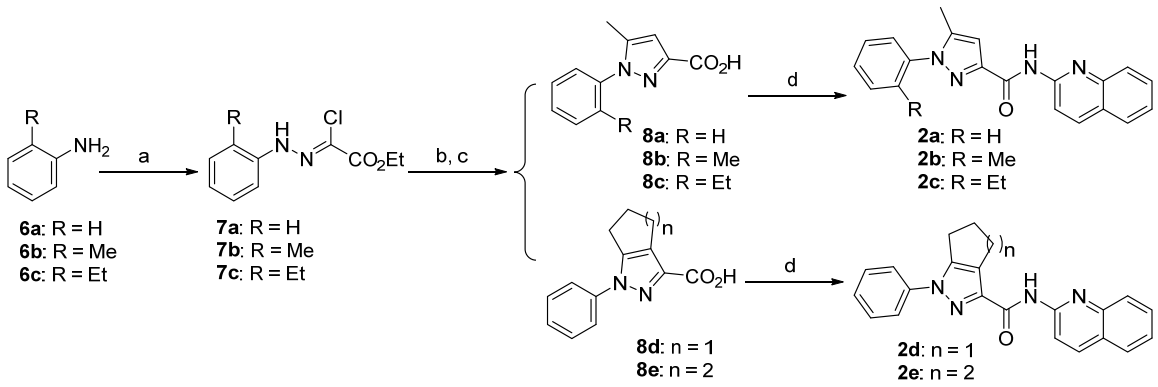

[a]Reagents and conditions: (a) i) $NaNO_2$, HCl (aq.), 0 °C; ii) ethyl 2-chloroacetoacetate NaOAc, EtOH/H_2O, 0-25 °C, 88-95%; (b) i) for **8a-c**, diethyl (2-oxopropyl)phosphonate, DME, LiOH, rt, 10 h; for **8d-e**, ii) 4-(cyclopent-1-en-1-yl)morpholine or 4-(cyclohex-1-en-1-yl)morpholine, Et_3N, 12 h, rt; (c) NaOH, MeOH, reflux, 70-85% for two steps; (d) 2-aminoquinoline, PyCIU, DIPEA, DCE, 80 °C, 63-71%.

Structure-Activity Relationship (SAR). The inhibitory potency of the synthesized compounds against the Wnt signaling pathway was determined using the Wnt-HEK293 luciferase gene reporter assay that was described previously (Table 1).[31] Compound 5-methyl-1-phenyl-*N*-(quinolin-2-yl)-1*H*-pyrazole-4-carboxamide (**1a**) had an IC_{50} value of 2.2 nM, which was similar to that of FX1128, while >300-fold and >200-fold more potent than pyrvinium and TNKS inhibitor XAV939, respectively. We then studied substitution effects on the phenyl ring. Replacement of the methyl group with an F atom resulted in a new inhibitor (**1b**) with excellent potency (IC_{50} = 0.92 nM), while with Br (**1c**) and Et (**1d**) groups at the same position yielded compounds with similarly good potencies. A second F (**1e**) or Br (**1f**) substituent at the *ortho*-position was well-tolerated. However, an additional halogen at the *para*- (**1g**) or *meta*-position (**1h**) was detrimental to the potency. The 2,5- and 2,6-dimethyl analogs (**1i-1j**) indicated IC_{50} values of 14 and 26 nM, respectively. These results indicated that single substituent at the *ortho*-position of the ring is preferred. Interestingly, inclusion of a nitrogen atom to the phenyl ring (**1k**) restored the high potency of the inhibitor, indicating that polar aromatic characteristics can be tolerated.

Next, the effect of R_1 on the pyrazole ring was studied. Replacing the Me group of **1a** with a Cl (**1l**) decreased the potency by 13 folds, while substitution of the Me group with larger Br (**1m**) or Et (**1n**) group retained high potency. However, further increase of the size to an *i*-Pr resulted in an analog (**1o**) with significantly decreased potency, although the similar sized *N*,*N*-dimethyl amino (**1p**) restored the potency of the compound.

Then we sought out to substitute the 2-aminoquinoline moiety using compound **1d** as a template. The naphthyl analog **1q** and its regio-isomer **1r** showed no obvious inhibitory activity at concentrations up to 1 μM. These results highlighted the importance of the presence and location of the quinoline nitrogen atom in maintaining high potency. Truncation of the quinoline yielded a new compound **1s**, which was >300-fold less potent than compound **1d**. This result demonstrated that the phenyl ring of the quinoline fragment was also critical.

Table 1. Inhibition of the Wnt/*β*-Catenin Signaling Pathway by Compounds 1a-s

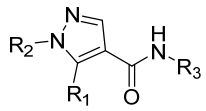

1a-s

compound	R_1	R_2	R_3	IC_{50} (nM)[a]
1a	Me		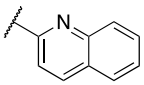	2.2 ± 0.3
1b	Me	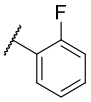	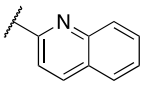	0.92 ± 0.1
1c (YW2065)	Me		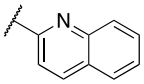	2.3 ± 0.4
1d	Me	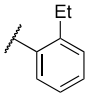	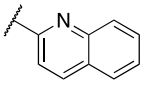	1.2 ± 0.3
1e	Me	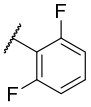	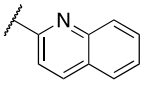	1.6 ± 0.3
1f	Me	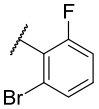	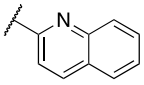	3.2 ± 0.6

1g	Me	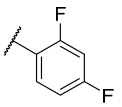	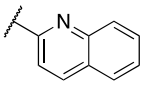	16 ± 1
1h	Me	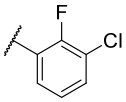	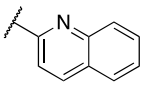	14 ± 3.1
1i	Me	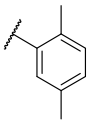	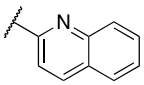	14 ± 1.3
1j	Me		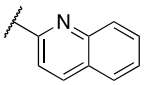	26 ± 0.9
1k	Me		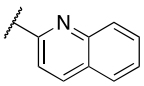	2.2 ± 0.3
1l	Cl		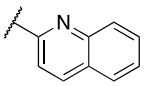	29 ± 5
1m	Br		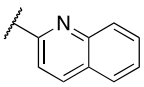	3.7 ± 0.3
1n	Et		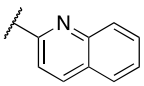	1.7 ± 0.3
1o	*i*-Pr		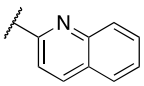	15 ± 1
1p	$N(CH_3)_2$		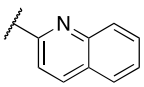	6.0 ± 1.5
1q	Me		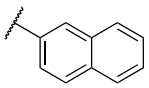	>1,000
1r	Me	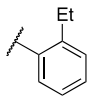	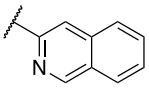	>1,000
1s	Me	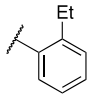	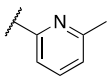	380 ± 5
pyrvinium				750 ± 137

XAV939	450 ± 130

[a]The values of IC_{50} for each compound were calculated and data are expressed as mean IC_{50} (nM) ± SD from three independent experiments.

We have also synthesized and tested the regioisomers of the pyrazole core (**2a-e**). As shown in Table 2, compounds **2a-e** indicated significantly decreased potency compared to the ones in Table 1. These results indicated that the position of the amide substitution on the pyrazole core plays a critical role in the inhibitory activity of inhibitors.

Table 2. Inhibition of the Wnt/*β*-Catenin Signaling Pathway by Compounds 2a-e

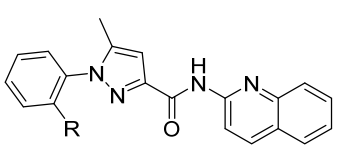

2a-c

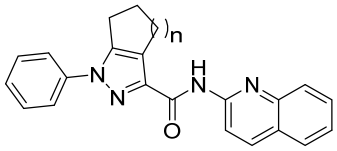

2d-e

compound	R	n	IC_{50} (nM)[a]
2a	H	-	637 ± 67
2b	Me	-	250 ± 13
2c	Et	-	67 ± 9
2d	H	1	140 ± 4
2e	H	2	260 ± 42

[a]The IC_{50} values were calculated and data are expressed as mean IC_{50} (nM) ± SD from three independent experiments.

Next, compounds **1a**-**1p**, which showed promising potencies in the luciferase gene reporter assays, were further tested for their activities in killing human CRC SW480 cells

(Figure 3A). Nine compounds that showed over 50% growth inhibition at 50 μM were then tested in full dose responses to obtain their GI_{50} values (Figure 3B). Compounds **1c** (YW2065) and **1f** demonstrated good potencies with GI_{50} values of 2.4 μM and 3.9 μM, respectively. The TANK inhibitor XAV939 indicated a GI_{50} value of >50 μM. Note that GI_{50} values of our new inhibitors in this CRC cell killing assays were significantly higher than the corresponding IC_{50} values obtained from the gene reporter assays. We reasoned that the reporter assay was designed with high sensitivity and respond rapidly to perturbations of the Wnt signaling pathway. However, when the compounds were tested in killing the much more complex cancer cells, the effects usually took a longer time to take place. Therefore, we observed significantly decreased sensitivities of inhibitors in killing the SW480 cells. Moreover, the effects of Wnt inhibition can be alleviated by the function of other biological pathways, which might also contribute to the delayed cell death.

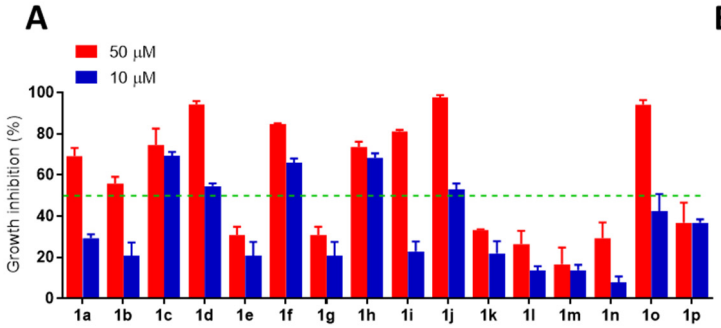

B

Compound	GI_{50} SW480 (μM)
1a	23.9 ± 2.2
1b	33.3 ± 1.0
1c (YW2065)	2.4 ± 0.1
1d	9.7 ± 1.2
1f	3.9 ± 0.2
1h	9.0 ± 1.5
1i	24.6 ± 7.1
1j	7.2 ± 0.5
1o	17.3 ± 4.4
pyrvinium	3.7 ± 0.1
XAV939	>50

Figure 3. (A) Anti-proliferation activity of selected compounds on the growth of SW480 cells. (B) The GI_{50} values were calculated and data was expressed as mean GI_{50} (μM) ± SD from three independent experiments.

Encouraged by the activity of YW2065 in both luciferase gene reporter assay and CRC cell killing assay, we next studied the mechanism of action of this compound (Figure 4). Similar to pyrvinium and FX1128, YW2065 induced *β*-catenin degradation in HEK293 cells (Figure 4B). Interestingly, YW2065 was found to enhance the expression of Axin-1 in fluorescent imaging (Figure 4A) and western blot analysis (Figure 4B). Axin-1 is not only a master scaffolding protein for the destruction complex of *β*-catenin, but also a key regulator of multiple pathways. It was reported that Axin-1 enhances AMPK activation through the Axin-LKB1-AMPK complex, which facilitates the Thr172 phosphorylation and subsequent activation of AMPK.[43] To verify the relationship between Axin-1 and AMPK, we overexpressed Axin-1 in HEK293 cells and found that the overexpression of Axin-1 led to increased AMPK phosphorylation (Figure 4C). Similar activation of AMPK was also observed when HEK293 cells were exposed to compound YW2065 and several analogs, while the effect was abolished by Axin-1 knockdown (Figure 4D, Figure S2). These results suggested that YW2065 achieved its dual activities of Wnt inhibition and AMPK activation through the mechanism of Axin-1 stabilization. Note that TNKS inhibitors (e.g., XAV939) also function by stabilizing Axin. However, our previous results showed that the YW2065 analog FX1128 did not bind to TNKS in SPR binding assay.[31] More importantly, TNKS inhibitor XAV939 failed to activate AMPK.[31,44] These data highlighted that YW2065 achieved dual activities of Wnt inhibition and AMPK activation through Axin-1 stabilization via a novel mechanism different from TNKS inhibitors. The mechanism for YW2065 to activate AMPK is also likely different from

those of other known AMPK activators such as metformin, AICAR and salicylates. Whereas metformin and AICAR activate AMPK *via* the disruption of the adenylate charge in the cell, salicylates directly act on the AMPK β1-subunit.[45,46] Currently additional investigations are undergoing to elucidate whether YW2065 stabilized Axin-1 through direct binding or other indirect mechanism.

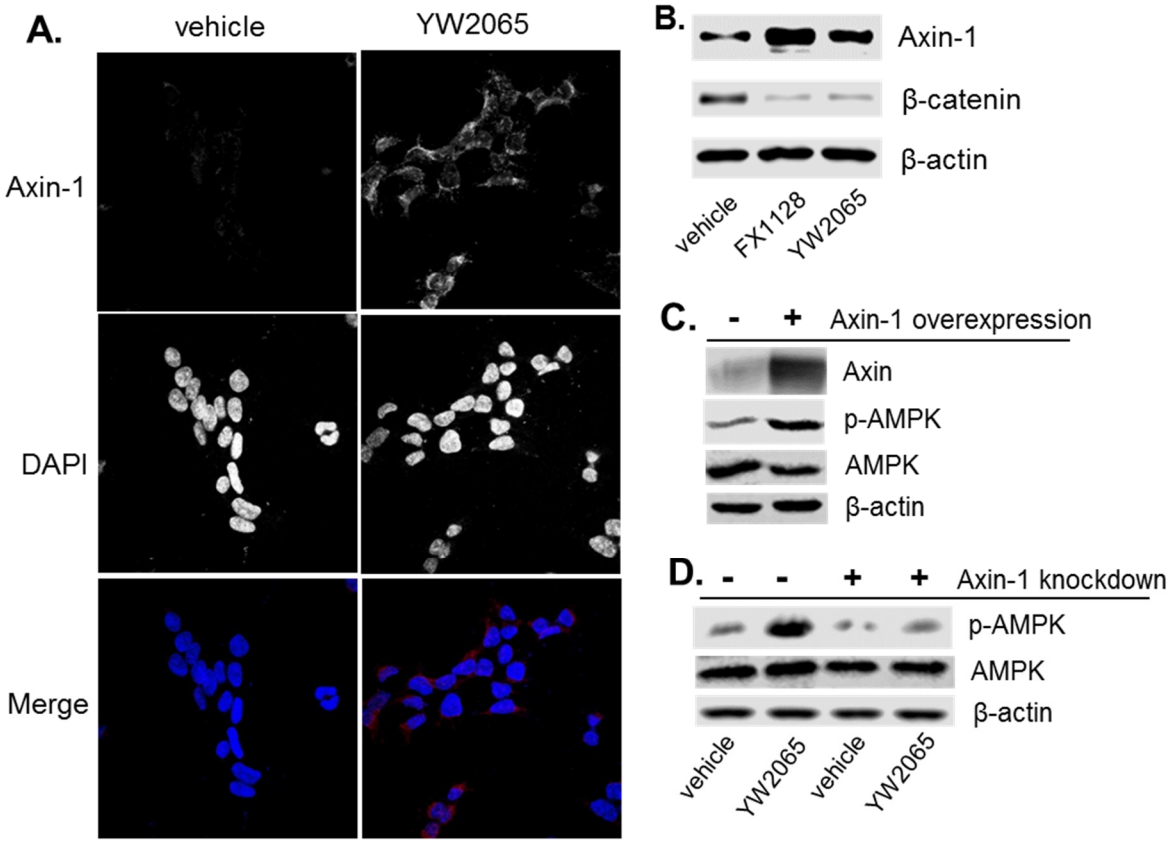

Figure 4. Dual function of YW2065 for Wnt signaling inhibition and AMPK activation. (A) Enhanced Axin-1 protein expression by YW2065 (1 μM) treatment. HEK293 cells were stained with anti-Axin-1 antibody and DAPI, and the images were taken under fluorescence microscopy. (B) Enhanced Axin-1 expression and increased *β*-catenin degradation by YW2065 or its analog FX1128 in HEK293 cells. (C) Increased AMPK

phosphorylation by Axin-1 overexpression (empty pcDNA 3 *vs.* pcDNA3-Axin-1) in HEK293 cells. (D) Axin-1 knockdown abolished the effect of AMPK activation by YW2065 in HEK293 cells.

Next, the activity of YW2065 was further investigated using human CRC SW480 and SW620 cells (Figure 5). SW480 and SW620 cells are derived from the primary and metastatic sites of the same patient, respectively. Both cells contain hyperactivated Wnt signaling pathway. Similar to the results from gene reporter assays using HEK293 cells (Table 1), YW2065 demonstrated excellent inhibitory potencies (IC_{50} = 1.15 nM and 0.19 nM, respectively) in the TOPflash reporter assays using both SW480 and SW620 cells (Figure 5A). Because the lymph node metastatic site derived SW620 cells have been widely used as a mCRC cellular model, additional Western blot and RT-PCR analyses were performed using this cell line. Upon treatment of YW2065, the protein level of Axin-1 was increased dose-dependently, while the protein level of β-catenin was significantly decreased (Figure 5B). We also confirmed that the mRNA levels of Wnt target genes, including *c-Myc*, *cyclin D1, MMP7,* and *S100A4*, were significantly decreased upon the treatment of YW2065 (Figure 5C). Moreover, YW2065 activated AMPK through phosphorylation, which in turn, led to the phosphorylation of the downstream substrate acetyl-CoA carboxylase (ACC) in a dose-dependent manner (Figure 5D). These results confirmed YW2065's dual activities of Wnt inhibition and AMPK activation in CRC cells.

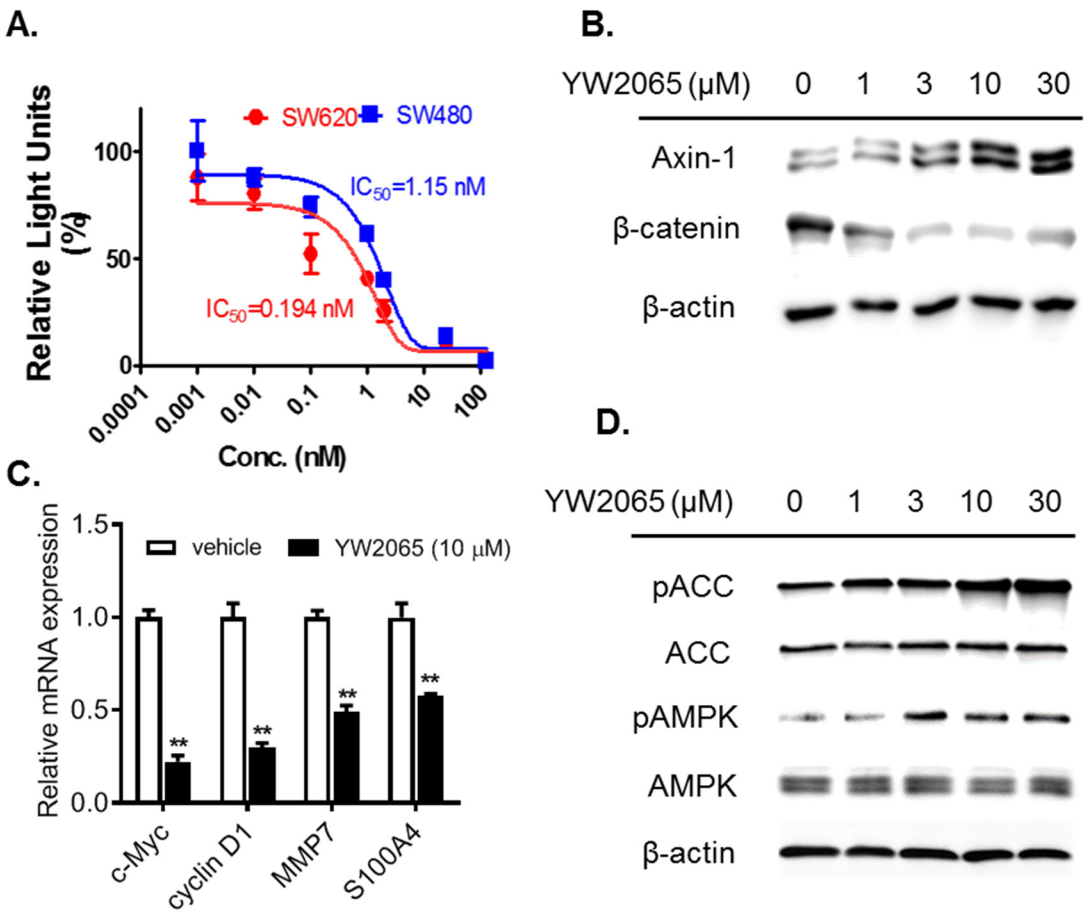

Figure 5. Inhibition of Wnt/*β*-catenin pathway and activation of AMPK by YW2065 in CRC cells. (A) TOPflash reporter assay was performed in SW480 and SW620 cells. (B) Dose response of *β*-catenin and Axin-1 levels upon treatment of YW2065. (C) Decreased mRNA levels of Wnt target genes in SW620 cells upon exposure to YW2065 for 24 h. (D) Dose response of AMPK and ACC phosphorylation upon the treatment of YW2065.

To characterize the *in vitro* anti-CRC activities of YW2065, we performed the colony formation assay using SW480, SW620, and an additional human CRC HT29 cell

lines (Figure 6A). The results showed that compound YW2065 dose-dependently inhibited the colony formation of all three cell lines. In addition, as analyzed by flow cytometry, treatment of YW2065 dose-dependently caused apoptosis in all three CRC cells (Figure 6B and data not shown). Importantly, SW620 cells became resistant to the cytotoxicity of YW2065 when constitutively active *β*-catenin mutant (S33Y) was overexpressed, or the Axin-1 gene was knocked down (Figure 6C). These results were in consistent with the mechanistic engagement of Wnt signaling as a critical part of the action of YW2065.

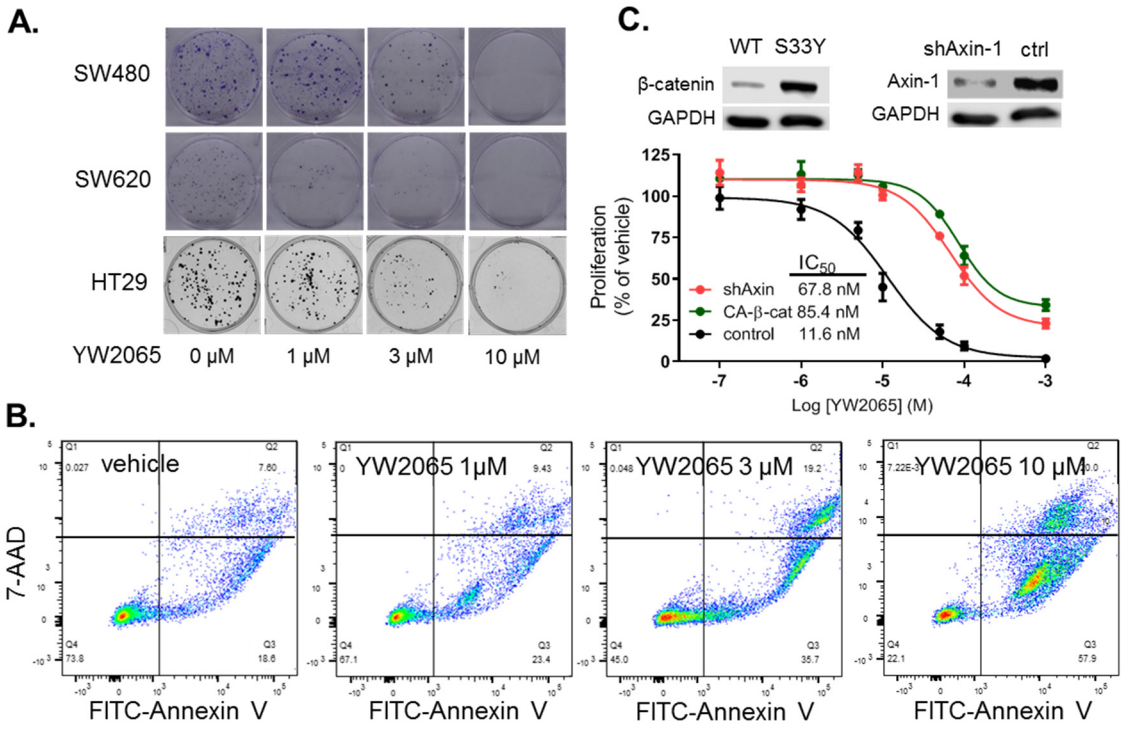

Figure 6. YW2065 inhibited CRC cell proliferation and growth *in vitro*. (A) Inhibition of colony formation of CRC cells by YW2065 treatment. Cells (500 cells/well in 6-well plate) were treated with vehicle or YW2065 until visible colonies formed. (B) Induction

of apoptosis by YW2065 treatment in SW620 cells. SW620 cells were treated with YW2065 for 48 h, then stained with AAD-7 and annexin V, then analyzed by flow cytometry. (C) SW620 cells became resistant to YW2065 cytotoxicity when Axin-1 was knocked down by lentivrus encoding shRNA against Axin-1 or a constitutively active *β*-catenin mutant (S33Y) was overexpressed. Cells were treated with YW2065 or vehicle for 72 h.

To further study target specificity of YW2065, it was tested against a panel of 273 kinases. The results indicated that YW2065 inhibited none of the tested kinases with over 40% at the concentration of 1000 nM. It displayed a moderate inhibitory activity (39% inhibition) for RPS6KA3, and weak activities against 10 other kinases including CDK17, GSK3A, MAP4K4, MAPKAPK3, MELK, NEK6, NTRK1, PAK3, PRKCQ, and SRC (Table S1).

Next, the pharmacokinetic (PK) profile of compound YW2065 was determined (Table 3). Compound YW2065 was administrated as a single dose at 5 mg/kg, either intravenously (I.V.) or orally (P.O.). The maximum serum concentration (C_{max}) was determined to be approximately 5 μg/mL, and the T_{max} was measured to be around 18 min. Compared to the extremely low bioavailability of pyrvinium, the bioavailability (F%) of YW2065 was improved to be about 23%. The area under the curve (AUC) values of I.V. and P.O. were calculated to be 57.5 μg·h/ mL and 13.2 μg·h/ mL, respectively. Finally, the half-life ($T_{1/2}$) of compound YW2065 was determined to be about 3 h.

Table 3. Single Dose Pharmacokinetics of YW2065.[a]

Route of Administration	I.V. (n = 3)	P.O. (n = 5)
Dose (mg/kg)	5.0	5.0
C_{max} (μg/mL)		5.2 ± 2.6
T_{max} (min)		18.0 ± 6.7
F (%)		22.9 ± 9.3
$AUC_{(0\text{-inf})}$ (μg·h/mL)	57.5 ± 16.1	13.2 ± 3.8
$T_{1/2}$ (h)	3.1 ± 1.5	2.9 ± 1.6

[a]Pharmacokinetic parameters of YW2065 derived from Phoenix WinNonlin 7.3 using the non-compartmental analysis. Data is presented as estimates average ± standard deviation.

Considering the favorable PK properties of YW2065, we proceeded to evaluate its anti-CRC efficacy *in vivo* using an SW620 tumor xenograft mice model (Figure 7).[47] SW620 cells were implanted subcutaneously in the female nude mice on the right flank. After tumors reached a volume of 100-200 mm^2, mice (n = 6/group) received YW2065 (10 mg/kg or 50 mg/kg) or vehicle intraperitoneally (I.P.). Compound YW2065 reduced both tumor volume (Figure 7A) and final tumor weight (Figure 7B). The tumor volume in the high dosage group (50 mg/kg/day) was decreased by 49% compared to the vehicle group in the last measurement. In addition, YW2065 was also well tolerated based on body weight and liver/kidney function tests (Figures S3-S4). Mouse body weight gain showed no significant difference in the control and YW2065 treated groups. In a 21-day toxicity test at a dose of 100 mg/kg/day (I.P.), minimal system toxicity of compound YW2065 was observed. To assess *β*-catenin inhibition and AMPK activation, the tumor tissues were harvested and subjected to western blot and RT-PCR analysis. Compared to the samples

from vehicle group, the phosphorylation of AMPK and ACC was increased in those from the YW2065-treated group (Figure 7C). In addition, the transcripts of Wnt target genes *Axin-2, MMP-7* and *S100A4* were reduced upon treatment of compound YW2065 (Figure 7D). It should be noted that the tolerability and efficacy of YW2065 has yet to be fully elucidated in the context of systemic exposure for specific routes of dosing. Nevertheless, as proof of concepts, we have demonstrated that YW2065 has exhibited an improved pharmacokinetic properties as compared to the parent pyrvinium and importantly, the therapeutic effects against *in vivo* colon cancer growth.

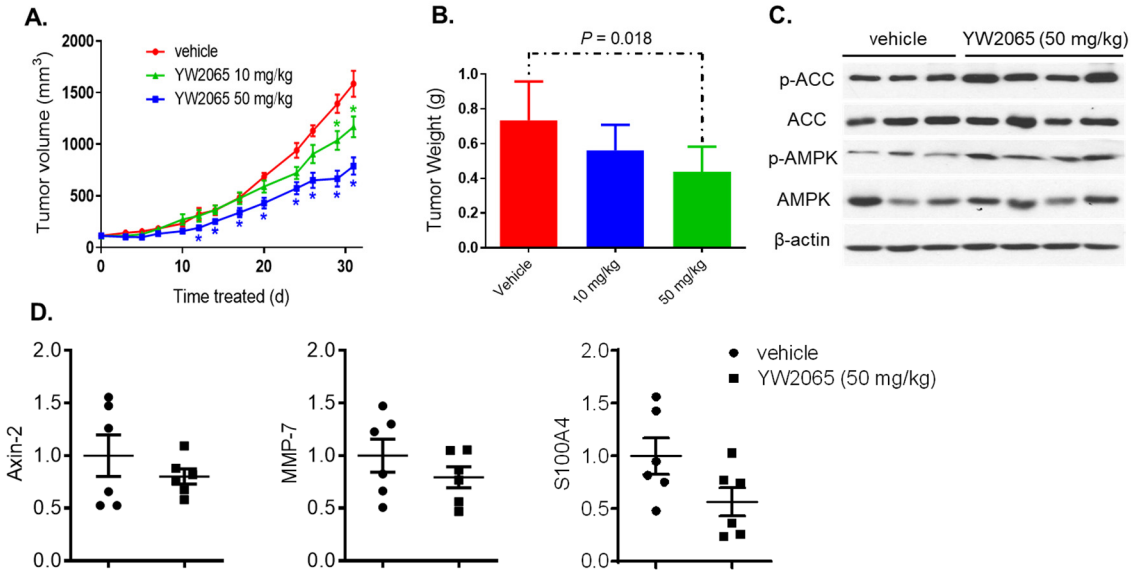

Figure 7. YW2065 suppressed SW620 tumor growth *in vivo*. Six-week old nude mice were injected with 2×10^6 SW620 cells subcutaneous. After tumors reach a volume of 100-200 mm^2, mice were received I.P. injection of vehicle or 10 mg/kg, 50 mg/kg of YW2065 each day (n = 6 each group). The tumor growth (A) was measured every other

day. *$P < 0.05$ as compared to the vehicle control in t test. The mice were euthanized at day 32, and tumors were weighed (B). The phosphorylation of AMPK and ACC in the tumor tissues was detected by western blot (C). The expression of Wnt pathway target genes (*Axin-2*, *MMP-7*, and *S100A4*) in tumor tissues were detected by RT-PCR (D).

CONCLUSIONS

The mCRC, with complex genetic profiles and poor prognoses, remains a significant cause of cancer related morbidity worldwide. We reported a series of pyrazole-based small molecules that displayed potent anti-CRC activities *in vitro* and *in vivo*. One of the compounds, YW2065, displayed dual activities of Wnt inhibition and AMPK activation, which was convergent by Axin-1 stabilization. Moreover, YW2065 demonstrated favorable PK properties and suppressed tumor growth in a xenograft mouse model. Therefore, YW2065 represents a promising new lead for further development of anti-CRC therapeutics.

EXPERIMENTAL SECTION

Chemical Analysis. All chemicals were obtained from commercial suppliers and used without further purification. Analytical thin layer chromatography was visualized by ultraviolet light at 256 nM. ^{1}H NMR spectra were recorded on a Varian (400 MHz) spectrometer. Data are presented as follows: chemical shift (in ppm on the δ scale relative to δ = 0.00 ppm for the protons in tetramethylsilane (TMS)), integration, multiplicity (s = singlet, d = doublet, t = triplet, q = quartet, m = multiplet, br = broad), coupling constant (*J*/Hz). ^{13}C NMR spectra were recorded at 100 MHz, and all chemical shifts values are reported in ppm on the δ scale with an internal reference of δ 77.0 or 39.0 for $CDCl_3$ or DMSO-d_6, respectively. The purities of title compounds were determined by analytic HPLC, performed on an Agilent 1100 instrument and a reverse-phase column (Waters XTerrra RP18, 5 μM, 4.6 × 250 mm). All compounds were eluted with 45% acetonitrile/55% water (containing 0.1% TFA) over 20 mins with a detection at 260 nM and a flow rate at 1.0 mL/min. All tested compounds were > 95% pure. Yields were not optimized. **4b-f** was commercially available. Pyrazole compounds **5e, 5f, 5l-p** and **8e** were prepared as reported previously. [48,49]

General Procedure A: Synthesis of Compounds 1a-s. To a solution of **5** (1.2 mmol), aromatic amines (1.0 mmol) in dichloroethane (5.0 mL) was added 1-(chloro-1-pyrrolidinylmethylene)pyrrolidinium hexafluorophosphate (398 mg, 1.2 mmol) and DIPEA (516 mg, 4 mmol). The mixture was allowed to stir at 80 °C overnight. The solvent

was removed under vacuum and the resulting residue was redissolved in ethyl acetate (15 mL). The resulting solution was washed with H_2O and brine, dried over Na_2SO_4 and concentrated. The crude material was purified by column chromatography to give compounds **1a-s** (24-88%).

5-Methyl-1-phenyl-*N*-(quinolin-2-yl)-1*H*-pyrazole-4-carboxamide (1a). The title compound was synthesized according to General Procedure A (81%): ^{1}H-NMR (400 MHz, $CDCl_3$) δ 8.74 (s, 1H), 8.55-8.53 (d, *J* = 9.6 Hz, 1H), 8.20-8.18 (d, *J* = 9.6 Hz, 1H), 8.09 (s, 1H), 7.84-7.82 (d, *J* = 8.8 Hz, 1H), 7.79-.77 (d, *J* = 8.0 Hz, 1H), 7.68-7.64 (t, *J* = 8.0 Hz, 1H), 7.53-7.49 (m, 2H), 7.47-7.43 (m, 4H), 2.66 (s, 3H); ^{13}C-NMR (100 MHz, $CDCl_3$) δ 162.2, 151.2, 146.4, 143.6, 138.6, 138.4, 130.1, 129.3, 128.8, 127.6, 127.0, 126.3, 125.5, 125.1, 115.4, 114.5, 12.1. HRMS $[M + H]^+$ (ESI-TOF) calcd for $C_{20}H_{17}N_4O$ 329.1402, found 329.1409. HPLC: t_R = 5.45 min, 99.9%.

1-(2-Fluorophenyl)-5-methyl-*N*-(quinolin-2-yl)-1*H*-pyrazole-4-carboxamide (1b). The title compound was synthesized according to General Procedure A (82%, a white solid) ^{1}H-NMR (400 MHz, DMSO-*d*$_6$) δ 10.93 (s, 1H), 8.64 (s, 1H), 8.39 (m, 2H). 7.96-7.94 (d, *J* = 8.0 Hz, 1H), 7.90-7.88 (d, *J* = 8.0 Hz, 1H), 7.55-7.71 (t, *J* = 8.0 Hz, 1H), 7.65-7.61 (m, 2H), 7.57-7.50 (m, 2H), 7.46-7.42 (t, *J* = 8.0 Hz, 1H), 2.46 (s, 3H); ^{13}C-NMR (100 MHz, DMSO-*d*$_6$) δ 167.5, 162.7, 160.2, 157.2, 151.6, 150.1, 145.8, 145.6, 143.1, 136.9, 136.8, 135.1, 134.6, 132.9, 132.1, 130.9, 130.6, 130.1, 122.0, 121.9, 120.6, 119.8, 16.2. HRMS $[M + H]^+$ (ESI-TOF) calcd for $C_{20}H_{16}FN_4O$ 347.1308, found 347.1300. HPLC: t_R = 5.83 min, 99.7%.

1-(2-Bromophenyl)-5-methyl-*N*-(quinolin-2-yl)-1*H*-pyrazole-4-carboxamide (1c, YW2065). The title compound was synthesized according to General Procedure A (65%, a yellow solid): ^{1}H-NMR (400 MHz, $CDCl_3$) δ 8.74 (s, 1H), 8.55-8.53 (d, *J* = 8.0 Hz, 1H), 8.20-8.18 (d, *J* = 8.8 Hz, 1H), 8.11 (s, 1H), 7.84-7.82 (d, *J* = 8.8 Hz, 1H), 7.79-7.77 (d, *J* = 8.8 Hz, 1H), 7.74-7.72 (d, *J* = 8.8 Hz, 1H), 7.68-7.64 (t, *J* = 8.0 Hz, 1H), 7.49-7.44 (m, 2H), 7.42-7.37 (m, 2H), 2.50 (s, 3H); ^{13}C-NMR (100 MHz, $CDCl_3$) δ 162.1, 151.2, 146.6, 145.2, 138.8, 138.5, 137.8, 133.6, 131.4, 130.0, 129.6, 128.4, 127.6, 127.2, 126.3, 125.1, 122.3, 114.8, 114.5, 11.4. HRMS $[M + H]^+$ (ESI-TOF) calcd for $C_{20}H_{15}BrN_4O$ 407.0507, found 407.0513. HPLC: t_R = 10.8 min, 100%.

1-(2-Ethylphenyl)-5-methyl-*N*-(quinolin-2-yl)-1*H*-pyrazole-4-carboxamide (1d). The title compound was synthesized according to General Procedure A (84%, a brown solid): ^{1}H-NMR (400 MHz, DMSO-d_6) δ 10.85 (s, 1H), 8.62 (s, 1H), 8.39 (m, 2H), 7.96-7.94 (d, *J* = 8.0 Hz, 1H), 7.90-7.88 (d, *J* = 8.0 Hz, 1H), 7.55-7.71 (t, *J* = 8.0 Hz, 1H), 7.53-7.50 (m, 3H), 7.42-7.38 (t, *J* = 8.0 Hz, 1H), 7.34-7.32 (d, *J* = 8.0 Hz, 1H), 2.36-2.31 (m, 5H), 1.03-1.0 (q, *J* = 8.0 Hz, 3H); ^{13}C-NMR (100 MHz, DMSO-d_6) δ 167.7, 157.2, 151.6, 149.4, 146.5, 144.7, 143.1, 142.1, 135.2, 135.1, 134.8, 133.0, 132.9, 132.1, 131.9, 130.8, 130.1, 120.6, 119.1, 28.6, 19.7, 16.5. HRMS $[M + H]^+$ (ESI-TOF) calcd for $C_{22}H_{21}N_4O$ 357.1715, found 357.1715. HPLC: t_R = 9.03 min, 99.2%.

1-(2,6-Difluorophenyl)-5-methyl-*N*-(quinolin-2-yl)-1*H*-pyrazole-4-carboxamide (1e). The title compound was synthesized according to General Procedure A (64%, a yellow foam): ^{1}H-NMR (400 MHz, $CDCl_3$) δ 8.91 (s, 1H), 8.53-8.51 (d, *J* = 9.6 Hz, 1H), 8.18 (s,

1H), 8.18-8.16 (d, *J* = 8.8 Hz, 1H), 7.82-7.80 (d, *J* = 8.4 Hz, 1H), 7.77-7.75 (d, *J* = 8.0 Hz, 1H), 7.65-7.61 (t, *J* = 7.2 Hz, 1H), 7.48-7.40 (m, 2H), 7.11-7.07 (t, *J* = 8.0 Hz, 1H), 2.53 (s, 3H); ^{13}C-NMR (100 MHz, $CDCl_3$) δ 161.9, 159.6, 157.1, 157.0, 151.2, 146.4, 139.9, 138.6, 131.6, 131.5, 131.4, 130.0, 127.6, 127.1, 126.3, 125.1, 115.2, 114.6, 112.5, 112.3, 10.9. HRMS $[M + H]^+$ (ESI-TOF) calcd for $C_{20}H_{15}F_2N_4O$ 365.1214, found 365.1210. HPLC: t_R = 7.08 min, 99.5%.

1-(2-Bromo-6-fluorophenyl)-5-methyl-*N*-(quinolin-2-yl)-1*H*-pyrazole-4-carboxamide (1f). The title compound was synthesized according to General Procedure A (69%, a white solid): ^{1}H-NMR (400 MHz, $CDCl_3$) δ 8.89 (s, 1H), 8.55-8.53 (d, *J* = 8.8 Hz, 1H), 8.20-8.18 (t, *J* = 4.8 Hz, 2H), 7.83-7.81 (d, *J* = 8.0 Hz, 1H), 7.78-7.76 (d, *J* = 8.8 Hz, 1H), 7.67-7.63 (t, *J* = 8.0 Hz, 1H), 7.54-7.52 (d, *J* = 8.0 Hz, 1H), 7.45-7.41 (t, *J* = 8.0 Hz, 1H), 7.40-7.35 (m, 1H), 7.25-7.21 (t, *J* = 8.0 Hz, 1H), 2.50 (s, 3H); ^{13}C-NMR (100 MHz, $CDCl_3$) δ 161.9, 160.2, 157.6, 151.2, 146.5, 145.9, 139.7, 138.6, 132.3, 132.2, 130.1, 128.9, 127.6, 127.1, 126.5, 126.3, 125.1, 123.9, 115.9, 115.8, 115.1, 114.6, 10.9. HRMS $[M + H]^+$ (ESI-TOF) calcd for $C_{20}H_{15}BrFN_4O$ 425.0413, found 425.0416. HPLC: t_R = 9.03min, 99.9%.

1-(2,4-Difluorophenyl)-5-methyl-*N*-(quinolin-2-yl)-1*H*-pyrazole-4-carboxamide (1g). The title compound was synthesized according to General Procedure A (82%, a brown solid): ^{1}H-NMR (400 MHz, $CDCl_3$) δ 8.75 (s, 1H), 8.54-8.52 (d, *J* = 8.8 Hz, 1H), 8.22-8.20 (d, *J* = 8.8 Hz, 1H), 8.14 (s, 1H), 7.84-7.82 (d, *J* = 8.8 Hz, 1H), 7.81-7.79 (d, *J* = 8.8 Hz, 1H), 7.69-7.65 (t, *J* = 8.8 Hz, 1H), 7.50-7.44 (m, 2H), 7.06-7.02 (m, 2H), 2.55 (s, 3H); ^{13}C-NMR (100 MHz, $CDCl_3$) δ 164.4, 164.3, 161.9, 158.4, 155.7, 151.1, 146.4, 145.6,

139.4, 138.7, 130.1, 130.0, 127.6, 127.0, 126.3, 125.2, 115.2, 114.5, 112.4, 112.2, 105.4, 105.2, 104.9, 11.2. HRMS $[M + H]^+$ (ESI-TOF) calcd for $C_{20}H_{15}F_2N_4O$ 365.1214, found 365.1202. HPLC: t_R = 6.07 min, 99.8%.

1-(3-Chloro-2-fluorophenyl)-5-methyl-*N*-(quinolin-2-yl)-1*H*-pyrazole-4-carboxamide (1h). The title compound was synthesized according to General Procedure A (56%, a white solid): ^{1}H-NMR (400 MHz, $CDCl_3$) δ 8.70 (s, 1H), 8.54-8.52 (d, *J* = 8.4 Hz, 1H), 8.22-8.20 (d, *J* = 8.8 Hz, 1H), 8.14 (s, 1H), 7.84-7.82 (d, *J* = 8.8 Hz, 1H), 7.81-7.79 (d, *J* = 8.0 Hz, 1H), 7.69-7.65 (t, *J* = 7.2 Hz, 1H), 7.58-7.54 (t, *J* = 7.2 Hz, 1H), 7.48-7.44 (t, *J* = 7.2 Hz, 1H), 7.41-7.37 (t, *J* = 7.2 Hz, 1H), 7.28-7.24 (t, *J* = 8.0 Hz, 1H), 2.58 (s, 3H); ^{13}C-NMR (100 MHz, $CDCl_3$) δ 161.8, 154.2, 151.6, 151.1, 146.5, 145.6, 139.5, 138.6, 131.8, 130.1, 127.6, 127.3, 127.2, 126.3, 125.2, 124.9, 124.8, 122.7, 115.4, 114.5, 11.3. HRMS $[M + H]^+$ (ESI-TOF) calcd for $C_{20}H_{15}ClFN_4O$ 381.0918, found 381.0928. HPLC: t_R = 10.21 min, 99.8%.

1-(2,5-Dimethylphenyl)-5-methyl-*N*-(quinolin-2-yl)-1*H*-pyrazole-4-carboxamide (1i). The title compound was synthesized according to General Procedure A (56%, a yellow oil): ^{1}H-NMR (400 MHz, $CDCl_3$) δ 8.84 (s, 1H), 8.56-8.54 (d, *J* = 8.8 Hz, 1H), 8.20-8.18 (d, *J* = 8.8 Hz, 1H), 8.11 (s, 1H), 7.84-7.82 (d, *J* = 8.8 Hz, 1H), 7.79-7.77 (d, *J* = 8.8 Hz, 1H), 7.68-7.64 (t, *J* = 8.0 Hz, 1H), 7.46-7.42 (t, *J* = 8.0 Hz, 1H), 7.21-7.18 (m, 2H), 7.04 (s, 1H), 2.45 (s, 3H), 2.35 (s, 3H), 1.98 (s, 3H); ^{13}C-NMR (100 MHz, $CDCl_3$) δ 162.4, 151.3, 146.4, 144.4, 138.6, 138.4, 137.3, 136.7, 132.5, 130.9, 130.6, 130.0, 127.6, 127.1, 126.2, 125.1,

114.6, 114.4, 20.7, 16.7, 11.3. HRMS $[M + H]^+$ (ESI-TOF) calcd for $C_{22}H_{21}N_4O$ 357.1715, found 357.1728. HPLC: t_R = 8.39 min, 99.9%.

1-(2,6-Dimethylphenyl)-5-methyl-*N*-(quinolin-2-yl)-1*H*-pyrazole-4-carboxamide (1j). The title compound was synthesized according to General Procedure A (74%, a yellow foam): ^{1}H-NMR (400 MHz, DMSO-*d*$_6$) δ 10.85 (s, 1H), 8.67 (s, 1H), 8.39 (m, 2H), 7.96-7.94 (d, *J* = 8.0 Hz, 1H), 7.90-7.88 (d, *J* = 8.0 Hz, 1H), 7.76-7.72 (t, *J* = 8.0 Hz, 1H), 7.54-7.50 (t, *J* = 8.0 Hz, 1H), 7.40-7.36 (t, *J* = 8.0 Hz, 1H), 7.29-7.27 (m, 2H), 2.29 (s, 3H), 1.91 (s, 6H); ^{13}C-NMR (100 MHz, DMSO-*d*$_6$) δ 167.7, 157.2, 151.6, 149.1, 145.2, 143.1, 141.8, 141.1, 135.1, 134.8, 133.5, 132.9, 132.1, 130.8, 130.1, 120.6, 119.1, 21.9, 15.8. HRMS $[M + H]^+$ (ESI-TOF) calcd for $C_{22}H_{21}N_4O$ 357.1715, found 357.1714. HPLC: t_R = 7.82 min, 99.6%.

5-Methyl-1-(3-methylpyridin-2-yl)-*N*-(quinolin-2-yl)-1*H*-pyrazole-4-carboxamide (1k). The title compound was synthesized according to General Procedure A (24%, a white solid): ^{1}H-NMR (400 MHz, $CDCl_3$) δ 8.55 (s, 1H), 8.53 (s, 1H), 8.47-8.46 (d, *J* = 4.0 Hz, 1H), 8.21-8.19 (d, *J* = 8.8 Hz, 1H), 8.01 (s, 1H), 7.85-7.83 (d, *J* = 8.0 Hz, 1H), 7.81-7.79 (d, *J* = 8.0 Hz, 1H), 7.77-7.75 (d, *J* = 8.0 Hz, 1H), 7.70-7.66 (t, *J* = 8.0 Hz, 1H), 7.47-7.43 (t, *J* = 8.0 Hz, 1H), 7.39-7.36 (m, 1H), 2.58 (s, 3H), 2.20 (s, 3H); ^{13}C-NMR (100 MHz, $CDCl_3$) δ 162.1, 151.1, 150.0, 146.7, 144.7, 140.6, 138.5, 131.0, 130.0, 127.6, 127.3, 126.3, 125.1, 124.8, 114.9, 114.5, 17.2, 11.4. HRMS $[M + H]^+$ (ESI-TOF) calcd for $C_{20}H_{18}N_5O$ 344.1511, found 344.1507. HPLC: t_R = 3.73 min, 99.6%.

5-Chloro-1-phenyl-*N*-(quinolin-2-yl)-1*H*-pyrazole-4-carboxamide (1l). The title

compound was synthesized according to General Procedure A (55%, a white solid): ^{1}H-NMR (400 MHz, $CDCl_3$) δ 8.93 (s, 1H), 8.53 (s, 1H), 8.27 (s, 1H), 8.22-8.20 (d, *J* = 8.0 Hz, 1H), 7.86-7.84 (d, *J* = 8.0 Hz, 1H), 7.80-7.78 (d, *J* = 8.0 Hz, 1H), 7.68-7.64 (t, *J* = 8.0 Hz, 1H), 7.55-7.45 (m, 5H); ^{13}C-NMR (100 MHz, $CDCl_3$) δ 159.5, 150.8, 141.6, 139.9, 138.7, 138.6, 130.0, 129.6, 129.4, 129.2, 127.4, 126.5, 126.1, 125.3, 119.5, 115.3, 114.6. HRMS $[M + H]^+$ (ESI-TOF) calcd for $C_{19}H_{14}ClN_4O$ 349.0856, found 349.0652. HPLC: t_R = 13.58 min, 99.0%.

5-Bromo-1-phenyl-*N*-(quinolin-2-yl)-1*H*-pyrazole-4-carboxamide (1m). The title compound was synthesized according to General Procedure A (60%, a white solid): ^{1}H-NMR (400 MHz, $CDCl_3$) δ 8.94 (s, 1H), 8.56-8.54 (d, *J* = 8.0 Hz, 1H), 8.29 (s, 1H), 8.22-8.20 (d, *J* = 8.0 Hz, 1H), 7.87-7.85 (d, *J* = 8.4 Hz, 1H), 7.81-7.79 (d, *J* = 8.0 Hz, 1H), 7.70-7.66 (t, *J* = 8.0 Hz, 1H), 7.54 (m, 5H), 7.48-7.44 (d, *J* = 8.0 Hz, 1H); ^{13}C-NMR (100 MHz, $CDCl_3$) δ 161.0, 150.8, 142.1, 138.7, 138.2, 130.0, 129.5, 129.2, 127.6, 127.4, 126.5, 126.2, 125.3, 119.6, 117.9, 114.8, 114.6. HRMS $[M + H]^+$ (ESI-TOF) calcd for $C_{19}H_{14}BrN_4O$ 393.0351, found 393.0355. HPLC: t_R = 13.12 min, 99.2%.

5-Ethyl-1-phenyl-*N*-(quinolin-2-yl)-1*H*-pyrazole-4-carboxamide (1n). The title compound was synthesized according to General Procedure A (66%, a white solid): ^{1}H-NMR (400 MHz, $CDCl_3$) δ 8.66 (s, 1H), 8.55-8.53 (d, *J* = 9.6 Hz, 1H), 8.20-8.18 (d, *J* = 9.6 Hz, 1H), 8.06 (s, 1H), 7.85-7.83 (d, *J* = 8.4 Hz, 1H), 7.80-7.78 (d, *J* = 8.0 Hz, 1H), 7.69-7.65 (t, *J* = 8.0 Hz, 1H), 7.54-7.43 (m, 6H), 3.09-3.04 (q, *J* = 8.0 Hz, 2H), 1.25-1.21 (t, *J* = 8.0 Hz, 3H); ^{13}C-NMR (100 MHz, $CDCl_3$) δ 161.8, 151.2, 149.6, 146.7, 138.8, 138.5,

138.5, 130.0, 129.3, 129.1, 127.6, 127.2, 126.3, 125.9, 125.1, 114.5, 18.7, 13.7. HRMS [M + H]$^+$ (ESI-TOF) calcd for $C_{21}H_{19}N_4O$ 343.1559, found 343.1558. HPLC: t_R = 3.63 min, 95.0%.

5-Isopropyl-1-phenyl-*N*-(quinolin-2-yl)-1*H*-pyrazole-4-carboxamide (1o). The title compound was synthesized according to General Procedure A (56%, a white solid): ^{1}H-NMR (400 MHz, $CDCl_3$) δ 8.83 (s, 1H), 8.55-8.53 (d, *J* = 8.4 Hz, 1H), 8.19-8.17 (d, *J* = 8.8 Hz, 1H), 8.00 (s, 1H), 7.83-7.81 (d, *J* = 8.8 Hz, 1H), 7.79-7.77 (d, *J* = 8.0 Hz, 1H), 7.66-7.62 (t, *J* = 8.0 Hz, 1H), 7.51-7.49 (m, 3H), 7.45-7.41 (t, *J* = 8.0 Hz, 1H), 7.39-7.37 (d, *J* = 7.2 Hz, 2H), 3.35-3.31 (m, 1H), 1.42-1.40 (d, *J* = 7.2 Hz, 6H); ^{13}C-NMR (100 MHz, $CDCl_3$) δ 162.1, 152.6, 151.4, 146.7, 139.4, 138.5, 129.9, 129.3, 129.2, 127.6, 127.2, 126.6, 126.3, 125.0, 114.8, 114.5, 26.5, 20.5. HRMS [M + H]$^+$ (ESI-TOF) calcd for $C_{22}H_{20}N_4O$ 357.1715, found 357.1719. HPLC: t_R = 12.86 min, 99.9%.

5-(Dimethylamino)-1-phenyl-*N*-(quinolin-2-yl)-1*H*-pyrazole-4-carboxamide (1p). The title compound was synthesized according to General Procedure A (80%, a white solid): ^{1}H-NMR (400 MHz, $CDCl_3$) δ 9.81 (s, 1H), 8.59-8.57 (d, *J* = 8.8 Hz, 1H), 8.19-8.17 (d, *J* = 8.8 Hz, 1H), 8.15 (s, 1H), 7.86-7.84 (d, *J* = 8.0 Hz, 1H), 7.79-7.77 (d, *J* = 8.8 Hz, 1H), 7.67-7.63 (t, *J* = 8.0 Hz, 1H), 7.55-7.46 (m, 5H), 7.45-7.41 (t, *J* = 8.0 Hz, 1H), 2.84 (s, 6H); ^{13}C-NMR (100 MHz, $CDCl_3$) δ 161.1, 151.4, 150.5, 146.8, 141.2, 139.7, 138.3, 129.8, 129.3, 129.1, 127.5, 127.4, 126.3, 125.7, 124.8, 114.7, 109.5, 43.1. HRMS [M + H]$^+$ (ESI-TOF) calcd for $C_{21}H_{20}N_5O$ 358.1668, found 358.1666. HPLC: t_R = 12.40 min, 97.8%.

1-(2-Ethylphenyl)-5-methyl-*N*-(naphthalen-2-yl)-1*H*-pyrazole-4-carboxamide (1q).

The title compound was synthesized according to General Procedure A (80%): ^{1}H-NMR (400 MHz, $CDCl_3$) δ 8.29 (s, 1H), 8.19 (s, 1H), 8.06 (s, 1H), 7.78-7.76 (m, 3H), 7.58-7.56 (d, *J* = 8.0 Hz, 1H), 7.46-7.38 (m, 4H), 7.31-7.27 (t, *J* = 8.0 Hz, 1H), 7.17-7.15 (d, *J* = 8.0 Hz, 1H), 2.42 (s, 3H), 2.38-2.32 (q, *J* = 8.0 Hz, 2H), 1.10-1.06 (t, *J* = 8.0 Hz, 3H); ^{13}C-NMR (100 MHz, $CDCl_3$) δ 162.3, 144.2, 141.8, 137.9, 136.9, 135.6, 133.9, 130.6, 130.1, 129.5, 128.6, 127.7, 127.5, 126.7, 126.4, 124.9, 120.4, 117.0, 114.9, 23.9, 14.4, 11.4. HRMS $[M + H]^+$ (ESI-TOF) calcd for $C_{23}H_{22}N_3O$ 356.1763, found 356.1766. HPLC: t_R = 12.83 min, 98.0%.

1-(2-Ethylphenyl)-*N*-(isoquinolin-3-yl)-5-methyl-1*H*-pyrazole-4-carboxamide (1r). The title compound was synthesized according to General Procedure A (82%): ^{1}H-NMR (400 MHz, $CDCl_3$) δ 8.98 (s, 1H), 8.70 (s, 1H), 8.65 (s, 1H), 8.08 (s, 1H), 7.88-7.7.86 (d, *J* = 8.8 Hz, 1H), 7.83-7.81 (d, *J* = 8.8 Hz, 1H), 7.64-7.60 (t, *J* = 8.0 Hz, 1H), 7.47-7.43 (m, 2H), 7.40-7.38 (d, *J* = 8.0 Hz, 1H), 7.33-7.29 (t, *J* = 7.2 Hz, 1H), 7.21-7.19 (d, *J* = 8.4 Hz, 1H), 2.47 (s, 3H), 2.39-2.34 (q, *J* = 7.2 Hz, 2H), 1.10-1.06 (t, *J* = 7.2 Hz, 3H); ^{13}C-NMR (100 MHz, $CDCl_3$) δ 161.9, 151.1, 146.5, 144.2, 141.8, 138.0, 136.9, 130.8, 130.0, 129.5, 127.7, 126.8, 126.7, 126.4, 125.7, 114.6, 107.9, 23.9, 14.4, 11.5. HRMS $[M + H]^+$ (ESI-TOF) calcd for $C_{22}H_{21}N_4O$ 357.1715, found 357.1709. HPLC: t_R = 10.40 min, 99.9%.

1-(2-Ethylphenyl)-5-methyl-*N*-(6-methylpyridin-2-yl)-1*H*-pyrazole-4-carboxamide (1s). The title compound was synthesized according to General Procedure A (88%): ^{1}H-NMR (400 MHz, $CDCl_3$) δ 8.52 (s, 1H), 8.12-8.10 (d, *J* = 8.0 Hz, 1H), 8.00 (s, 1H), 7.60-7.56 (t, *J* = 8.0 Hz, 1H), 7.43-7.39 (t, *J* = 8.0 Hz, 1H), 7.37-7.35 (d, *J* = 8.0 Hz, 1H), 7.30-

7.26 (t, J = 8.0 Hz, 1H), 7.17-7.15 (d, J = 8.0 Hz, 1H), 6.87-6.85 (d, J = 8.0 Hz, 1H), 2.42 (s, 3H), 2.39 (s, 3H), 2.35-2.29 (q, J = 8.0 Hz, 2H), 1.06-1.02 (t, J = 8.0 Hz, 3H); ^{13}C-NMR (100 MHz, $CDCl_3$) δ 161.9, 156.7, 150.9, 144.3, 141.7, 138.6, 138.1, 136.9, 130.0, 129.5, 127.7, 126.6, 119.0, 114.5, 110.9, 23.9, 23.8, 14.4, 11.4. HRMS $[M + H]^+$ (ESI-TOF) calcd for $C_{19}H_{21}N_4O$321.1715, found 321.1712. HPLC: t_R = 5.18 min, 99.0%.

General Procedure B: Synthesis of Compounds 2a-e. Compounds **2a-e** were prepared from compound **8a-e** in a similar manner to that described for compounds **1a-s**.

5-Methyl-1-phenyl-*N*-(quinolin-2-yl)-1*H*-pyrazole-3-carboxamide (2a). The title compound was synthesized according to General Procedure B (71%, a white solid): ^{1}H-NMR (400 MHz, $CDCl_3$) δ 9.65 (s, 1H), 8.62-8.60 (d, J = 9.6 Hz, 1H), 8.21-8.18 (d, J = 9.6 Hz, 1H), 7.86-7.84 (d, J = 8.4 Hz, 1H), 7.79-7.77 (d, J = 8.8 Hz, 1H), 7.67-7.63 (t, J = 7.2 Hz, 1H), 7.56-7.41 (m, 6H), 6.86 (s, 1H), 2.39 (s, 3H); ^{13}C-NMR (100 MHz, $CDCl_3$) δ 160.6, 150.9, 146.8, 146.1, 141.4, 139.1, 138.4, 129.8, 129.2, 128.6, 127.5, 127.4, 126.3, 125.0, 124.9, 114.4, 107.8, 12.6. HRMS $[M + H]^+$ (ESI-TOF) calcd for $C_{20}H_{17}N_4O$ 329.1402, found 329.1406. HPLC: t_R = 20.42 min, 99.9%.

5-Methyl-*N*-(quinolin-2-yl)-1-(*o*-tolyl)-1*H*-pyrazole-3-carboxamide (2b). The title compound was synthesized according to General Procedure B (68%, a white solid): ^{1}H-NMR (400 MHz, $CDCl_3$) δ 9.63 (s, 1H), 8.61-8.59 (d, J = 9.6 Hz, 1H), 8.19-8.17 (d, J = 9.6 Hz, 1H), 7.82-7.80 (d, J = 8.8 Hz, 1H), 7.78-7.76 (d, J = 8.0 Hz, 1H), 7.65-7.61 (t, J = 7.2 Hz, 1H), 7.45-7.28 (m, 4H), 7.28-7.26 (d, J = 7.2 Hz, 1H), 6.86 (s, 1H), 2.16 (s, 3H), 2.08 (s, 3H); ^{13}C-NMR (100 MHz, $CDCl_3$) δ 160.7, 150.9, 146.9, 146.1, 142.2, 138.3, 137.8,

135.9, 131.2, 129.8, 129.7, 127.5, 127.4, 127.4, 126.8, 126.2, 124.9, 114.3, 106.3, 17.2, 11.5. HRMS $[M + H]^+$ (ESI-TOF) calcd for $C_{21}H_{19}N_4O$ 343.1559, found 343.1558. HPLC: t_R = 8.54 min, 99.9%.

1-(2-Ethylphenyl)-5-methyl-*N*-(quinolin-2-yl)-1*H*-pyrazole-3-carboxamide (2c). The title compound was synthesized according to General Procedure B (66%, a yellow solid): ^{1}H-NMR (400 MHz, $CDCl_3$) δ 9.63 (s, 1H), 8.62-8.60 (d, *J* = 8.8 Hz, 1H), 8.19-8.17 (d, *J* = 8.8 Hz, 1H), 7.8-7.80 (d, *J* = 8.8 Hz, 1H), 7.77-7.75 (d, *J* = 8.0 Hz, 1H), 7.64-7.60 (t, *J* = 7.2 Hz, 1H), 7.50-7.39 (m, 3H), 7.37-7.33 (t, *J* = 7.6 Hz, 1H), 7.25-7.23 (d, *J* = 8.0 Hz, 1H), 6.86 (s, 1H), 2.44-2.40 (t, *J* = 8.0 Hz, 2H), 2.15 (s, 3H), 1.13-1.09 (d, *J* = 8.0 Hz, 3H); ^{13}C-NMR (100 MHz, $CDCl_3$) δ 160.7, 150.9, 146.9, 146.0, 142.4, 141.7, 138.3, 137.3, 130.1, 129.8, 129.6, 127.6, 127.5, 126.7, 126.2, 124.9, 114.3, 106.3, 23.9, 14.5, 11.6. HRMS $[M + H]^+$ (ESI-TOF) calcd for $C_{22}H_{21}N_4O$ 357.1715, found 357.1717. HPLC: t_R = 11.11 min, 99.7%.

1-Phenyl-*N*-(quinolin-2-yl)-1,4,5,6-tetrahydrocyclopenta[*c*]pyrazole-3-carboxamide. (2d). The title compound was synthesized according to General Procedure B (63%): ^{1}H-NMR (400 MHz, $CDCl_3$) δ 9.62 (s, 1H), 8.63-8.51 (d, *J* = 9.6 Hz, 1H), 8.19-8.17 (d, *J* = 8.8 Hz, 1H), 7.90-7.88 (d, *J* = 8.4 Hz, 1H), 7.79-7.77 (d, *J* = 8.0 Hz, 1H), 7.75-7.7.73 (d, *J* = 8.0 Hz, 1H), 7.69-7.65 (t, *J* = 8.0 Hz, 1H), 7.50-7.42 (m, 3H), 7.34-7.30 (t, *J* = 8.0 Hz, 1H), 3.05-3.01 (t, *J* = 7.2 Hz, 2H), 2.98-2.94 (t, *J* = 7.2 Hz, 2H), 2.71-2.66 (m, 2H); ^{13}C-NMR (100 MHz, $CDCl_3$) δ 160.9, 151.0, 150.9, 146.8, 139.9, 139.7, 138.4, 131.5, 129.9,

129.4, 127.5, 127.4, 126.8, 126.3, 124.9, 119.5, 114.3, 31.0, 26.8, 23.5. HRMS $[M + H]^+$ (ESI-TOF) calcd for $C_{22}H_{19}N_4O$ 355.1559, found 355.1564. HPLC: t_R = 13.14 min, 99.8%.

1-Phenyl-*N*-(quinolin-2-yl)-4,5,6,7-tetrahydro-1*H*-indazole-3-carboxamide (2e). The title compound was synthesized according to General Procedure B (65%): ^{1}H-NMR (400 MHz, $CDCl_3$) δ 9.69 (s, 1H), 8.63-8.61 (d, *J* = 8.8 Hz, 1H), 8.18-8.16 (d, *J* = 8.8 Hz, 1H), 7.87-7.85 (d, *J* = 8.8 Hz, 1H), 7.77-7.75 (d, *J* = 8.0 Hz, 1H), 7.66-7.64 (d, *J* = 8.0 Hz, 1H), 7.67-7.63 (t, *J* = 8.0 Hz, 1H), 7.57-7.55 (d, *J* = 8.0 Hz, 2H), 7.52-7.48 (t, *J* = 8.0 Hz, 2H), 7.43-7.40 (m, 2H), 2.97 (m, 2H), 2.73 (m, 2H), 1.82 (m, 4H); ^{13}C-NMR (100 MHz, $CDCl_3$) δ 161.6, 151.1, 146.9, 142.4, 140.9, 139.2, 138.3, 129.8, 129.2, 127.7, 127.5, 127.4, 126.2, 124.8, 123.5, 120.6, 114.3, 23.8, 22.6, 22.4, 21.6. HRMS $[M + H]^+$ (ESI-TOF) calcd for $C_{23}H_{21}N_4O$ 369.1715, found 369.1717. HPLC: t_R = 14.85 min, 99.9%.

(*E*)-Ethyl 2-((dimethylamino)methylene)-3-oxobutanoate (4a). To a solution of ethyl acetoacetate (2.6 g, 20 mmol) in ethanol (10 mL) was added *N,N*-Dimethylformamide dimethyl acetal (2.5 g, 21 mmol). The mixture was allowed to stir at 60 ºC for 3 h, then cooled to room temperature and concentrated under vacuum to give a crude product **5a** (3.6 g, 97%), which was used without further purification.

General Procedure C: Synthesis of Compounds 5a-p. To a solution of **4a-f** (19.5 mmol) in ethanol (20 mL) was added DIPEA (2.71 g, 21 mmol) and substituted hydrazine (21 mmol). The mixture was allowed to stir at 60 ºC for 3 h. Then, the mixture was cooled to room temperature, concentrated to give the crude product as an oil, which was used in the next step without further purification.

To the above crude material (10 mmol) in EtOH (20 mL) was added a solution of NaOH (50 mmol) in H_2O (5 mL). The resulting reaction mixture was heated under reflux for 2 h, then cooled to room temperature and concentrated. The resulting aqueous solution was neutralized using HCl (1 N). The precipitate was filtered, washed with H_2O, and dried under vacuum at 50 °C to afford compounds **5a**-**p** (40-98%).

5-Methyl-1-phenyl-1*H*-pyrazole-4-carboxylic acid (5a). The title compound was synthesized according to General Procedure C (80%). ^{1}H-NMR (400 MHz, DMSO-d_6) δ 12.45 (s, 1H), 7.98 (s, 1H), 7.59-7.49 (m, 5H), 2.51 (s, 3H); ^{13}C-NMR (100 MHz, DMSO-d_6) δ 169.7, 148.4, 146.8, 143.8, 134.5, 133.7, 130.5, 118.2, 16.7.

1-(2-Fluorophenyl)-5-methyl-1*H*-pyrazole-4-carboxylic acid (5b). The title compound was synthesized according to General Procedure C (94%). ^{1}H-NMR (400 MHz, DMSO-d_6) δ 12.56 (s, 1H), 8.03 (s, 1H), 7.64-7.58 (m, 2H), 7.53-7.748 (t, J = 8.8 Hz, 1H), 7.43-7.39 (t, J = 8.8 Hz, 1H), 2.37 (s, 3H); ^{13}C-NMR (100 MHz, DMSO-d_6) δ 169.5, 162.9, 160.2, 149.9, 147.3, 136.9, 136.8, 134.5, 130.5, 130.5, 122.0, 121.8, 117.9, 15.8.

1-(2-Bromophenyl)-5-methyl-1*H*-pyrazole-4-carboxylic acid (5c). The title compound was synthesized according to General Procedure C (98%). ^{1}H-NMR (400 MHz, DMSO-d_6) δ 12.45 (s, 1H), 7.99 (s, 1H), 7.89-7.87 (d, J = 8.0 Hz, 1H), 7.61-7.54 (m, 3H), 2.28 (s, 3H); ^{13}C-NMR (100 MHz, DMSO-d_6) δ 169.6, 149.5, 146.8, 142.7, 138.5, 137.0, 135.2, 134.1, 126.6, 117.5, 16.0.

1-(2-Ethylphenyl)-5-methyl-1*H*-pyrazole-4-carboxylic acid (5d). The title compound was synthesized according to General Procedure C (78%). ^{1}H-NMR (400 MHz, DMSO-

*d*6) δ 12.41 (s, 1H), 7.98 (s, 1H), 7.53-7.47 (m, 2H), 7.40-7.36 (t, *J* = 8.0 Hz, 1H), 7.32-7.30 (d, *J* = 8.0 Hz, 1H), 2.29-2.67 (m, 5H), 1.00-0.96 (t, *J* = 8.0 Hz, 3H); ^{13}C-NMR (100 MHz, DMSO-*d*6) δ 169.7, 149.2, 146.4, 146.4, 142.0, 135.1, 134.8, 132.9, 131.9, 117.1, 28.6, 19.6, 16.2.

1-(2,4-Difluorophenyl)-5-methyl-1*H*-pyrazole-4-carboxylic acid (5g). The title compound was synthesized according to General Procedure C (83%). ^{1}H-NMR (400 MHz, DMSO-*d*6) δ 12.49 (s, 1H), 8.01 (s, 1H), 7.72-7.66 (m, 1H), 7.62-7.56 (m, 1H), 7.33-7.29 (m, 1H), 2.36 (s, 3H); ^{13}C-NMR (100 MHz, DMSO-*d*6) δ 169.5, 168.9, 168.8, 166.4, 166.3, 163.3, 163.1, 160.7, 160.6, 150.2, 147.4, 136.0, 135.9, 117.9, 117.8, 117.6, 117.6, 110.8, 110.5, 110.3, 15.8.

1-(3-Chloro-2-fluorophenyl)-5-methyl-1*H*-pyrazole-4-carboxylic acid. (5h) The title compound was synthesized according to General Procedure C (86%). ^{1}H-NMR (400 MHz, DMSO-*d*6) δ 12.45 (s, 1H), 8.04 (s, 1H), 7.84-7.80 (t, *J* = 7.2 Hz, 1H), 7.63-7.59 (t, *J* = 7.2 Hz, 1H), 7.46-7.42 (t, *J* = 7.2 Hz, 1H), 2.38 (s, 3H); ^{13}C-NMR (100 MHz, DMSO-*d*6) δ 169.4, 158.7, 156.1, 150.2, 147.6, 137.1, 133.5, 132.6, 132.5, 131.0, 130.9, 126.2, 126.0, 118.1, 15.9.

1-(2,5-Dimethylphenyl)-5-methyl-1*H*-pyrazole-4-carboxylic acid (5i). The title compound was synthesized according to General Procedure C (75%). ^{1}H-NMR (400 MHz, DMSO-*d*6) δ 12.11 (s, 1H), 7.96 (s, 1H), 7.31-7.29 (d, *J* = 8.0 Hz, 1H), 7.26-7.24 (d, *J* = 8.0 Hz, 1H), 7.13 (s, 1H), 2.32 (s, 3H), 2.26 (s, 3H), 1.90 (s, 3H); ^{13}C-NMR (100 MHz, DMSO-*d*6) δ 169.8, 148.9, 146.4, 142.5, 141.5, 137.3, 135.9, 135.5, 133.1, 117.1, 25.4,

21.4, 15.9.

1-(2,6-Dimethylphenyl)-5-methyl-1*H*-pyrazole-4-carboxylic acid (5j). The title compound was synthesized according to General Procedure C (48%). ^{1}H-NMR (400 MHz, DMSO-*d*$_6$) δ 12.44 (s, 1H), 8.01 (s, 1H), 7.39-7.35 (t, *J* = 8.0 Hz, 1H), 7.27-7.25 (d, *J* = 8.0 Hz, 1H), 2.20 (s, 3H), 1.88 (s, 6H); ^{13}C-NMR (100 MHz, DMSO-*d*$_6$) δ 169.8, 148.9, 146.9, 141.8, 141.0, 134.8, 133.5, 117.0, 21.9, 15.4.

5-Methyl-1-(3-methylpyridin-2-yl)-1*H*-pyrazole-4-carboxylic acid. (5k) The title compound was synthesized according to General Procedure C (48%**).** ^{1}H-NMR (400 MHz, DMSO-*d*$_6$) δ 12.27 (s, 1H), 8.47-8.46 (d, *J* = 4.0 Hz, 1H), 7.99-7.96 (m, 2H), 7.56-7.53 (m, 1H), 2.37 (s, 3H), 2.11 (s, 3H); ^{13}C-NMR (100 MHz, DMSO-*d*$_6$) δ 169.6, 154.9, 151.7, 149.1, 146.6, 146.1, 135.8, 130.3, 117.5, 21.8, 16.0.

General Procedure D: Synthesis of Compounds 7a-c. A solution of aniline (0.11 mol), concentrated HCl (28 mL), EtOH (14 mL), and H_2O (14 mL) was cooled at -5 °C, and then a solution of sodium nitrite (8.28 g, 0.12 mol) in H_2O (38 mL) was added dropwise while the temperature was maintained below 5 °C. A cold solution of ethyl 2-chloroacetoacetate (18.1 g, 15.2 mL, 0.11 mol), sodium acetate trihydrate (22.5 g, 1.27 mol) in EtOH (270 mL), and H_2O (30 mL) was added, and the reaction was stirred at -5 °C for 4 h. The reaction was quenched with H_2O (4 L) and kept stirring overnight. The solid was collected and recrystallized from EtOH to give compounds **7a-c**.

(*Z*)-Ethyl 2-chloro-2-(2-phenylhydrazono)acetate (7a). The title compound was synthesized according to General Procedure D (95%, a yellow solid): ^{1}H-NMR (400 MHz,

$CDCl_3$) δ 8.40 (s, 1H), 7.35-7.31(t, *J* = 8.0 Hz, 2H), 7.24-7.22 (d, *J* = 8.0 Hz, 2H), 7.06-7.02 (t, *J* = 8.0 Hz, 1H), 4.41-4.36 (q, *J* = 7.2 Hz, 2H), 1.42-1.38 (t, *J* = 7.2 Hz, 3H); ^{13}C-NMR (100 MHz, $CDCl_3$) δ 159.7, 141.6, 129.4, 123.1, 115.9, 114.5, 62.8, 14.2.

(*Z*)-Ethyl 2-chloro-2-(2-(o-tolyl)hydrazono)acetate (7b). The title compound was synthesized according to General Procedure D (88%, a yellow solid): ^{1}H-NMR (400 MHz, $CDCl_3$) δ 8.27 (s, 1H), 7.56-7.54 (d, *J* = 8.0 Hz, 1H), 7.26-7.22 (t, *J* = 8.0 Hz, 1H), 7.26-7.22 (t, *J* = 8.0 Hz, 1H), 7.15-7.13 (d, *J* = 8.0 Hz, 1H), 4.43-4.37 (q, *J* = 7.2 Hz, 2H), 2.31 (s, 3H), 1.43-1.39 (t, *J* = 7.2 Hz, 3H); ^{13}C-NMR (100 MHz, $CDCl_3$) δ 159.7, 139.4, 130.7, 127.4, 122.8, 122.3, 116.8, 114.5, 62.8, 16.7, 14.2.

(*Z*)-Ethyl 2-chloro-2-(2-(2-ethylphenyl)hydrazono)acetate (7c). The title compound was synthesized according to General Procedure D (90%, a yellow solid): ^{1}H-NMR (400 MHz, $CDCl_3$) δ 8.39 (s, 1H), 7.58-7.56 (d, *J* = 8.0 Hz, 1H), 7.26-7.22 (t, *J* = 8.0 Hz, 1H), 7.17-7.15 (d, *J* = 8.0 Hz, 1H), 7.03-6.99 (t, *J* = 8.0 Hz, 1H), 4.42-4.37 (q, *J* = 7.2 Hz, 2H), 2.68-2.62 (q, *J* = 8.0 Hz, 2H), 1.43-1.39 (t, *J* = 7.2 Hz, 3H), 1.32-1.28 (t, *J* = 8.0 Hz, 3H); ^{13}C-NMR (100 MHz, $CDCl_3$) δ 159.7, 138.8, 128.7, 128.3, 127.4, 123.1, 116.6, 114.9, 62.7, 23.6, 14.2, 13.4.

General Procedure E: Synthesis of Compounds 8a-c. Compound **7** (1.0 mmol) and diethyl (2-oxopropyl)phosphonate (1.0 mmol) were dissolved in DME (3 mL). LiOH (48 mg, 2.0 mmol) was added to the reaction mixture. The reaction mixture was allowed to stir at room temperature for 10 h. H_2O (6 mL) was added to the reaction mixture, the reaction mixture was then stirred overnight. Pyrazole-ester was then filtered, dried and used in the

next without further purification.

To pyrazole-ester (10 mmol) in EtOH (20 mL) was added a solution of NaOH (50 mmol) in H_2O (5 mL). The reaction was heated under reflux for 2 h, cooled to room temperature and concentrated. The resulting aqueous solution was neutralized by slow addition of HCl (1 N). The precipitate formed was filtered, washed with water and dried under vacuum at 50 °C to afford compounds **8a-c**.

5-Methyl-1-phenyl-1*H*-pyrazole-3-carboxylic acid (8a). The title compound was synthesized according to General Procedure E (85% for two steps): ^{1}H-NMR (400 MHz, $CDCl_3$) δ 7.51-7.47 m, 5H), 6.79 (s, 1H), 2.34 (s, 3H); ^{13}C-NMR (100 MHz, $CDCl_3$) δ166.3, 142.8, 141.0, 138.9, 129.2, 128.8, 125.3, 109.6, 12.4.

5-Methyl-1-(*o*-tolyl)-1*H*-pyrazole-3-carboxylic acid (8b). The title compound was synthesized according to General Procedure E (80% for two steps): ^{1}H-NMR (400 MHz, $CDCl_3$) δ 7.41-7.38 (t, J = 6.8 Hz, 1H), 7.34-7.32 (d, J = 8.4 Hz, 1H), 7.30-7.28 (d, J = 8.4 Hz, 1H), 7.26-7.22 (t, J = 6.8 Hz, 1H), 6.79 (s, 1H), 2.13 (s, 3H), 2.04 (s, 3H); ^{13}C-NMR (100 MHz, $CDCl_3$) δ 166.1, 142.7, 141.9, 137.7, 135.8, 131.0, 129.9, 127.5, 126.6, 108.2, 17.1, 11.4.

1-(2-Ethylphenyl)-5-methyl-1*H*-pyrazole-3-carboxylic acid (8c). The title compound was synthesized according to General Procedure E (70% for two steps): ^{1}H-NMR (400 MHz, $CDCl_3$) δ 7.47-7.43 (t, J = 6.8 Hz, 1H), 7.40-7.38 (d, J = 6.8.Hz, 1H), 7.33-7.29 (d, J = 6.8Hz, 1H), 7.22-7.02 (d, J = 7.6 Hz, 1H), 6.79 (s, 1H), 2.38-2.33 (q, J = 7.2 Hz, 2H),

2.14 (s, 3H), 1.10-1.06 (t, J = 7.2 Hz, 3H); ^{13}C-NMR (100 MHz, $CDCl_3$) δ 165.8, 142.6, 142.1, 141.6, 137.1, 130.1, 129.4, 127.6, 126.6, 108.2, 23.8, 14.3, 11.5.

1-Phenyl-1,4,5,6-tetrahydrocyclopenta[*c*]pyrazole-3-carboxylic acid (8d). In a three necked flask 6.7 g (0.04 mol) of freshly distilled enamine and 4.1 g (0.04 mol) of dry Et_3N were dissolved in dry chloroform (50 mL). A solution of phenylhydrazone (**7**), 10.8 g (0.04 mol), dissolved in chloroform (100 mL) was added dropwise at room temperature. The reaction mixture was stirred at room temperature for 12 h and then washed H_2O (3 ×). The organic layer was dried on dry Na_2SO_4. Evaporation of the solvent under reduced pressure yielded a thick oil which was used in the next step without further purification.

To obtained oil product (10 mmol) in EtOH (20 mL) was added a solution of NaOH (50 mmol) in H_2O (5 mL). The mixture was heated under reflux for 2 h. Then, the organic solvents were evaporated and the resulting aqueous phase was neutralized by slow addition of HCl (1 N). The precipitate formed was filtered, washed with water and dried under vacuum at 50 °C to afford compound **8d** as a brown solid (78% for two steps): ^{1}H-NMR (400 MHz, DMSO-d_6) δ 12.57 (s, 1H), 7.54-7.52 (d, J = 8.0 Hz, 2H), 7.37-7.33 (t, J = 8.0 Hz, 2H), 7.21-7.17 (t, J = 8.0 Hz, 1H), 2.89-2.85 (t, J = 7.2 Hz, 2H), 2.57-2.53 (t, J = 7.2 Hz, 2H), 2.42-2.34 (m, 2H); ^{13}C-NMR (100 MHz, DMSO-d_6) δ 168.3, 155.2, 144.4, 143.3, 136.7, 134.6, 131.9, 124.5, 35.3, 30.9, 28.4.

Cell Culture. HEK293, SW480, and HT29 cells were maintained in Dulbecco's Modified Eagle's Medium (DMEM) with fetal bovine serum (10%) and 1% PS (penicillin / streptomycin). SW620 cells were maintained in RPMI 1640 medium with fetal bovine

serum (10%) and 1% PS. All cells were incubated in 37 ˚C incubator with 5% CO_2.

Cell Proliferation Assay. Cells of log phase were used. 1000-3000 cells/well were seeded in 96-well plates with a volume of 100 μL. Cells were allowed to settle for 24 h in 37 ˚C incubators with 5% CO_2. Different concentration of 1000× stock solutions of the drug were made in DMSO. For IC_{50} determination, a 5-fold serial dilution of drugs started from 50 mM was used. The mixture (100 μL) was correspondingly added to the 96-well plate, each concentration had three replicates. DMSO instead of compound solution was used as the 0% inhibitor control. After incubation for 72 h, CCK-8 (10 μL) was added. Three hours later, the absorbance at 450 nm was measured. The data was calculated using GraphPad Prism. The IC_{50} were fitted using a nonlinear regression model with a sigmoidal dose response.

Wnt-HEK293 Luciferase Reporter Assay in a 1536-Well Plate Format. Stably transfected Wnt-HEK293 cells were dispensed at 2000/well in 4 μL of the Dulbecco's Modified Eagle Medium supplemented with 10% fetal bovine serum into white-solid 1,536-well plates (Greiner Bio-One North America Inc., Monroe, NC) using flying reagent dispenser (FRD, Aurora Discovery, San Diego, CA). The assay plates were incubated for overnight at 37 °C. Then 23 nL of test compounds were transferred to the assay plates using pintool station (Wako, San Diego, CA), followed by the addition of 1 μL of 200 ng/mL recombinant human Wnt-3a (R&D Systems Inc., Minneapolis, MN) using an FRD to all the wells except in the top half portions of the first four columns which received the control assay medium instead. The assay plates were incubated for 24 h at 37 °C. For

cell viability assay, 1 μL/well CellTiter-Fluor reagent (Promega Corporation, Madison, WI) was added using an FRD and fluorescence signal was measured through ViewLux plate reader (Perkin Elmer, Boston, MA) after 30 min incubation at 37 °C. For luciferase reporter assay, 4 μL/well ONE-Glo reagent (Promega Corporation) was added using an FRD and luminescence signal was measured through ViewLux plate reader after 30 min incubation at room temperature. Data were expressed as relative fluorescence units (cell viability assay) and relative luminescence units (luciferase reporter assay).

TCF/LEF Dual Luciferase Reporter Assay. SW480 and SW620 cells were seeded in 24-well plates at a density of 200,000 cells/well. Twenty four hours after seeding, transit transfections of TCF/LEF-Firefly luciferase expression construct (TOPflash, a gift from Randall Moon, Addgene plasmid #12456)[46] and pRLTK-Renilla vector were performed with lipofectamine 2000 (Invitrogen) according to the manufacturer`s instruction. After 16 h of transfection, the medium was change to new medium with different concentration of compounds, each concentration had three replicates. Twenty four hours later, luciferase activity was measured using dual luciferase reporter assay system (Promega) according to the manufacturer`s instruction.

Gene Overexpression and Knockdown. For overexpression and knockdown studies, the human pcDNA3-wild type and pcDNA3-S33Y β-catenin were gifts from Eric Fearon (Addgene plasmid #19286 and #16828), while the pLKO.1 control vector and shAxin plasmid were purchased from Sigma. The IC_{50} values were fitted using a nonlinear regression model with a sigmoidal dose response.

Western Blot. Cultured SW620 cells or tumor tissues were lysed with RIPA buffer containing protease inhibitor (Sigma). Protein concentrations were determined by DC protein assay kits (Bio-rad) and diluted to 2 mg/mL. Samples were denatured (98 °C for 5 min) and 20 μL loaded onto 7.5% SDS-PAGE protein gels for protein separation. After transferring to a nitrocellulose membrane, the membrane was blocked with 5% bovine serum albumin for 1 h. Primary rabbit antibody against either Axin-1 (1:1,000), *β*-catenin (1:2,000), Axin-2 (1:1,000), ACC (1:1,000), pACC (1:1,000), AMPK (1:1,000), pAMPK (1:1,000) or *β*-actin (1:2,000) was incubated overnight at 4 ˚C. Then HRP-linked rabbit secondary antibody (1:8000) was incubated for 2 h at room temperature. Blots were developed by enhanced chemiluminescence (Thermo) and images were taken using LICOR Odyssey® Fc Imaging System.

Colony Formation Assay. SW480, SW620 and HT29 cells were seeded in 6-well plates at a concentration of 300/well in medium (3 mL). Then, drugs at a series of concentrations were added. After 14 days, the plates were fixed with formaldehyde (4%), and stained with 0.5% crystal violet solution in MeOH aqueous solution (25%). Representative pictures of colonies were captured.

7-AAD/Annexin V Staining. SW620 cells (1×10^6) were seeded into 10 cm culture dish and recovered overnight. Different concentrations of compound YW2065 or DMSO were added for 48 h. The cells were harvested and stained with FITC Annexin V Apoptosis Detection Kit with 7-AAD (biolegend), according to manufacturer`s protocol.

Cell distribution was then analyzed by BD FACSCanto II Cytometer and processed by Flowjo software.

***In Vivo* Efficacy Study**. Female nude mice were purchased from the Jackson Laboratory. All procedures were carried out in accordance with NIH guidelines for animal experimentation and were approved by the Institutional Animal Care and Use Committee (IACUC) of the School of Medicine, University of Maryland Baltimore. SW620 cells (2×10^6) were injected subcutaneously into the right flank of each mouse. Mice were randomly grouped (6 mice/group) based on the tumor volume when the mean tumor volume reached 100−200 mm^3. YW2065 were dissolved in 10% DMSO, 10% Kolliphor, 80% saline. Mice were treated for 32 consecutive days via IP with YW2065 (50 mg/kg once daily, 10 mg/kg once daily), and vehicle, respectively. Tumor volume and body weight were monitored twice a week. Tumor volume was calculated as the L × W × W/2 (L and W are the length and width of the tumor, respectively). After the last measurement, mice were sacrificed and the tumors were separated for RNA extraction and western blot analyses.

Reverse Transcription and Real-time PCR. SW620 cells were seeded into 6-well plates and incubated for 24 h. Different concentrations of drugs were added to each well, each concentration had three replicates. After 24 h, cells were harvested and total RNA was isolated using Trizol and phenol-chloroform method. The total RNA (2 μg) was reversely transcribed using a high capability reverse transcript kit (Roche Applied Science). The RT-PCR was performed on ABI PRISM 7700 (Applied Biosystems). The following

primes were used: Axin-2: forward, 5′-TACACTCCTTATTGGGCGATCA; and reverse, 5′-TTGGCTACTCGTAAAGTTTTGGT; MMP-7: forward, 5′- GAGTGAGCTACAGTG GGAACA-3′; and reverse, 5′- CTATGACGCGGGAGTTTAACAT-3′; S100A4: forward, 5′- GATGAGCAACTTGGACAGCAA-3′; and reverse, 5′- CTGGGCTGCTTATCTGG GAAG-3′.

Pharmacokinetic Studies in Mice. Breeding pairs of C57BL/6J mice were purchased from Jackson Laboratory (Bar Harbor, ME) and housed in a room having temperature restraint of 21 ± 2 °C with humidity 60 ± 10% and maintained at 12 h light/dark cycle. The mice were provided with filtered water and food *ad libitum* and bred to produce offspring for our studies. For the PK experiments, male mice of 2-3 months weighing 23-26 grams (n=8) were used. All the procedures were carried out according to the NIH guidelines for animal experimentation and with the approval of the University of Maryland at Baltimore School of Medicine Institutional Animal Care and Use Committee. Each of the mice received 5 mg/kg of YW2065 prepared in 5% Kolliphor in saline; 3 mice were administered with this dosage intravenously and 5 *via* oral gavage. At six time points (0.25, 0.5, 1, 4, 8, 12 h), blood samples were collected from the tail vein of each mouse and immediately centrifuged at 8,000 rpm for 15 min to collect the plasma. Aliquots of the plasma sample were added to acetonitrile containing 0.5 μM of the internal standard (a YW2065 analog YW2013). The mixture was centrifuged at 13,000 rpm for 15 min, and the supernatant was analyzed with an ultra-performance liquid chromatography instrument (an Agilent 1200 series from Agilent Technologies, California) that is equipped with a

hybrid triple quadrupole 4000 QTRAP system (AB SCIEX, Massachusetts). The column used was a Cortecs C18+ 2.7 μm 2.1 x 75 mm column (Waters Corp., Milford, Massachusetts). Each sample was run for a total of 5 min with a gradient setup – 95% to 5% of mobile phase A over 1.5 min, 95% to 5% of B over 2 min, and 95% of A over 1.5 min. Mobile phase A was made up of 0.1% formic acid and 10 mM ammonium acetate in water while B was made up of 0.1% formic acid in acetonitrile. The ion transition used to detect YW2065 is 406.841 > 155.062 in the positive ion electrospray ionization (ES+) mode.

ASSOCIATED CONTENT

Supporting Information

The Supporting Information is available free of charge on the ACS Publication websites. SW480 cell viability assay for FX1128, mice weight gain study, 21-day mice toxicity study, HPLC trace for YW2065, and ^{1}H / ^{13}C NMR spectra of new compounds and molecular formula strings.

AUTHOR INFORMATION

Corresponding Authors

*For Y.S.: phone, 410-706-9324; Email: yshu@rx.umaryland.edu

*For F.X.: phone, 410-706-8521; Email: fxue@rx.umaryland.edu

Present Address

⊥School of Pharmaceutical Engineering, Jiangsu Food & Pharmaceutical Science College, Huaian, Jiangsu 223005, China (W.Y.).

Author Contributions

#These authors contributed equally to this work.

Notes

The authors declare no competing financial interest.

ACKNOWLEDGEMENTS

We thank the Maryland Innovation Initiative (MII) for the research grant to F.X. and Y.S., the Chinese National Natural Science Foundation [#21702073] to W.Y. and F.X. Dr. Yan Shu is a co-founder for and owns equity in Optivia Biotechnology. This work was supported in part by the Intramural Research Program of the National Center for Advancing Translational Sciences (NCATS).

ABBREVIATION USED

protein-protein interactions, PPI; colorectal cancer, CRC; vascular endothelial growth factor, VEGF; epidermal growth factor receptor, EGFR; adenomatous polyposis coli, APC; casein kinase 1α, CK1α; glycogen synthase kinase 3β, GSK3β; tankyrase, TNKS; CREB-binding protein, CBP; B cell CLL/lymphoma 9, BCL9; adenosine monophosphate (AMP)-activated protein kinase , AMPK; adenosine triphosphate, ATP; 5-aminoimidazole-4-carboxamide-ribonucleoside (AICAR); dimethylformamid-dimethylacetal, DMF-DMA; ethanol, EtOH; N,N-diisopropylethylamine, DIPEA; sodium hydroxide, NaOH; 1-(chloro-1-pyrrolidinylmethylene) pyrrolidinium, PyCIU; 1,2-dichloroethane, DCE; hydrochloric acid, HCl; sodium acetate, NaOAc; lithium hydroxide, LiOH; triethylamine, Et_3N; methanol MeOH; acetyl-CoA carboxylase (ACC).

REFERENCES

(1) Siegel, R. L.; Miller, K. D.; Jemal, A. Cancer statistics, 2015. *CA Cancer J. Clin.* **2015**, *65*, 5-29.

(2) Siegel, R.; Desantis, C.; Jemal, A. Colorectal cancer statistics, 2014. *CA Cancer J. Clin.* **2014**, *64*, 104-117.

(3) Chibaudel, B.; Tournigand, C.; Andre, T.; de Gramont, A. Therapeutic strategy in unresectable metastatic colorectal cancer. *Ther. Adv. Med. Oncol.* **2012**, *4*, 75-89.

(4) Gustavsson, B.; Carlsson, G.; Machover, D.; Petrelli, N.; Roth, A.; Schmoll, H. J.; Tveit, K. M.; Gibson, F. A review of the evolution of systemic chemotherapy in the management of colorectal cancer. *Clin. Colorectal Cancer* **2015**, *14*, 1-10.

(5) Venook, A. P. Epidermal growth factor receptor-targeted treatment for advanced colorectal carcinoma. *Cancer* **2005**, *103*, 2435-2446.

(6) Sun, W. Angiogenesis in metastatic colorectal cancer and the benefits of targeted therapy. *J. Hematol. Oncol.* **2012**, *5*, 63.

(7) Comprehensive molecular characterization of human colon and rectal cancer. *Nature* **2012**, *487*, 330-337.

(8) Clevers, H.; Nusse, R. Wnt/beta-catenin signaling and disease. *Cell* **2012**, *149*, 1192-1205.

(9) Bahrami, A.; Amerizadeh, F.; ShahidSales, S.; Khazaei, M.; Ghayour-Mobarhan, M.; Sadeghnia, H. R.; Maftouh, M.; Hassanian, S. M.; Avan, A. Therapeutic potential of targeting Wnt/beta-catenin pathway in treatment of colorectal cancer: rational and progress.

J. Cell. Biochem. **2017**, *118*, 1979-1983.

(10) Lu, B.; Green, B. A.; Farr, J. M.; Lopes, F. C.; Van Raay, T. J. Wnt drug discovery: weaving through the screens, patents and clinical trials. *Cancers* **2016**, *8,* 82.

(11) Zhang, X.; Hao, J. Development of anticancer agents targeting the Wnt/beta-catenin signaling. *Am. J. Cancer Res.* **2015**, *5*, 2344-2360.

(12) Lenz, H. J.; Kahn, M. Safely targeting cancer stem cells via selective catenin coactivator antagonism. *Cancer Sci.* **2014**, *105*, 1087-1092.

(13) Blagodatski, A.; Poteryaev, D.; Katanaev, V. L. Targeting the Wnt pathways for therapies. *Mol. Cell. Thera.* **2014**, *2*, 28.

(14) Liu, J.; Pan, S.; Hsieh, M. H.; Ng, N.; Sun, F.; Wang, T.; Kasibhatla, S.; Schuller, A. G.; Li, A. G.; Cheng, D.; Li, J.; Tompkins, C.; Pferdekamper, A.; Steffy, A.; Cheng, J.; Kowal, C.; Phung, V.; Guo, G.; Wang, Y.; Graham, M. P.; Flynn, S.; Brenner, J. C.; Li, C.; Villarroel, M. C.; Schultz, P. G.; Wu, X.; McNamara, P.; Sellers, W. R.; Petruzzelli, L.; Boral, A. L.; Seidel, H. M.; McLaughlin, M. E.; Che, J.; Carey, T. E.; Vanasse, G.; Harris, J. L. Targeting Wnt-driven cancer through the inhibition of porcupine by LGK974. *Proc. Natl. Acad. Sci. USA* **2013**, *110*, 20224-20229.

(15) Cheng, D.; Liu, J.; Han, D.; Zhang, G.; Gao, W.; Hsieh, M. H.; Ng, N.; Kasibhatla, S.; Tompkins, C.; Li, J.; Steffy, A.; Sun, F.; Li, C.; Seidel, H. M.; Harris, J. L.; Pan, S. Discovery of pyridinyl acetamide derivatives as potent, selective, and orally bioavailable porcupine inhibitors. *ACS Med. Chem. Lett.* **2016**, *7*, 676-680.

(16) Chen, B.; Dodge, M. E.; Tang, W.; Lu, J.; Ma, Z.; Fan, C.-W.; Wei, S.; Hao, W.; Kilgore,

J.; Williams, N. S.; Roth, M. G.; Amatruda, J. F.; Chen, C.; Lum, L. Small molecule–mediated disruption of Wnt-dependent signaling in tissue regeneration and cancer. *Nat. Chem. Biol.* **2009**, *5*, 100-107.

(17) Lepourcelet, M.; Chen, Y. N.; France, D. S.; Wang, H.; Crews, P.; Petersen, F.; Bruseo, C.; Wood, A. W.; Shivdasani, R. A. Small-molecule antagonists of the oncogenic Tcf/beta-catenin protein complex. *Cancer Cell* **2004**, *5*, 91-102.

(18) Gonsalves, F. C.; Klein, K.; Carson, B. B.; Katz, S.; Ekas, L. A.; Evans, S.; Nagourney, R.; Cardozo, T.; Brown, A. M.; DasGupta, R. An RNAi-based chemical genetic screen identifies three small-molecule inhibitors of the Wnt/wingless signaling pathway. *Proc. Natl. Acad. Sci. USA* **2011**, *108*, 5954-5963.

(19) Emami, K. H.; Nguyen, C.; Ma, H.; Kim, D. H.; Jeong, K. W.; Eguchi, M.; Moon, R. T.; Teo, J. L.; Kim, H. Y.; Moon, S. H.; Ha, J. R.; Kahn, M. A small molecule inhibitor of beta-catenin/CREB-binding protein transcription [corrected]. *Proc. Natl. Acad. Sci. USA* **2004**, *101*, 12682-12687.

(20) Huang, S. M.; Mishina, Y. M.; Liu, S.; Cheung, A.; Stegmeier, F.; Michaud, G. A.; Charlat, O.; Wiellette, E.; Zhang, Y.; Wiessner, S.; Hild, M.; Shi, X.; Wilson, C. J.; Mickanin, C.; Myer, V.; Fazal, A.; Tomlinson, R.; Serluca, F.; Shao, W.; Cheng, H.; Shultz, M.; Rau, C.; Schirle, M.; Schlegl, J.; Ghidelli, S.; Fawell, S.; Lu, C.; Curtis, D.; Kirschner, M. W.; Lengauer, C.; Finan, P. M.; Tallarico, J. A.; Bouwmeester, T.; Porter, J. A.; Bauer, A.; Cong, F. Tankyrase inhibition stabilizes axin and antagonizes Wnt signalling. *Nature* **2009**, *461*, 614-620.

(21) Voronkov, A.; Holsworth, D. D.; Waaler, J.; Wilson, S. R.; Ekblad, B.; Perdreau-Dahl, H.; Dinh, H.; Drewes, G.; Hopf, C.; Morth, J. P.; Krauss, S. Structural basis and SAR for G007-LK, a lead stage 1,2,4-triazole based specific tankyrase 1/2 inhibitor. *J. Med. Chem.* **2013**, *56*, 3012-3023.

(22) Shultz, M. D.; Cheung, A. K.; Kirby, C. A.; Firestone, B.; Fan, J.; Chen, C. H.; Chen, Z.; Chin, D. N.; Dipietro, L.; Fazal, A.; Feng, Y.; Fortin, P. D.; Gould, T.; Lagu, B.; Lei, H.; Lenoir, F.; Majumdar, D.; Ochala, E.; Palermo, M. G.; Pham, L.; Pu, M.; Smith, T.; Stams, T.; Tomlinson, R. C.; Toure, B. B.; Visser, M.; Wang, R. M.; Waters, N. J.; Shao, W. Identification of NVP-TNKS656: the use of structure-efficiency relationships to generate a highly potent, selective, and orally active tankyrase inhibitor. *J. Med. Chem.* **2013**, *56*, 6495-6511.

(23) Mariotti, L.; Templeton, C. M.; Ranes, M.; Paracuellos, P.; Cronin, N.; Beuron, F.; Morris, E.; Guettler, S. Tankyrase requires SAM domain-dependent polymerization to support Wnt-beta-catenin signaling. *Mol. Cell* **2016**, *63*, 498-513.

(24) Sbodio, J. I.; Chi, N. W. Identification of a tankyrase-binding motif shared by IRAP, TAB182, and human TRF1 but not mouse TRF1. NuMA contains this RXXPDG motif and is a novel tankyrase partner. *J. Biol. Chem.* **2002**, *277*, 31887-31892.

(25) Xu, D.; Liu, J.; Fu, T.; Shan, B.; Qian, L.; Pan, L.; Yuan, J. USP25 regulates Wnt signaling by controlling the stability of tankyrases. *Genes Dev.* **2017**, *31*, 1024-1035.

(26) Eisemann, T.; McCauley, M.; Langelier, M. F.; Gupta, K.; Roy, S.; Van Duyne, G. D.; Pascal, J. M. Tankyrase-1 ankyrin repeats form an adaptable binding platform for targets

of ADP-ribose modification. *Structure* **2016**, *24*, 1679-1692.

(27) Zhong, Y.; Katavolos, P.; Nguyen, T.; Lau, T.; Boggs, J.; Sambrone, A.; Kan, D.; Merchant, M.; Harstad, E.; Diaz, D.; Costa, M.; Schutten, M. Tankyrase inhibition causes reversible intestinal toxicity in mice with a therapeutic index < 1. *Toxicol. Pathol.* **2016**, *44*, 267-278.

(28) Mariotti, L.; Pollock, K.; Guettler, S. Regulation of Wnt/beta-catenin signalling by tankyrase-dependent poly(ADP-ribosyl)ation and scaffolding. *Br. J. Pharmacol.* **2017**, *174*, 4611-4636.

(29) Thorne, C. A.; Hanson, A. J.; Schneider, J.; Tahinci, E.; Orton, D.; Cselenyi, C. S.; Jernigan, K. K.; Meyers, K. C.; Hang, B. I.; Waterson, A. G.; Kim, K.; Melancon, B.; Ghidu, V. P.; Sulikowski, G. A.; LaFleur, B.; Salic, A.; Lee, L. A.; Miller, D. M.; Lee, E. Small-molecule inhibition of Wnt signaling through activation of casein kinase 1 alpha. *Nat. Chem. Biol.* **2010**, *6*, 829-836.

(30) Smith, T. C.; Kinkel, A. W.; Gryczko, C. M.; Goulet, J. R. Absorption of pyrvinium pamoate. *Clin. Pharmacol. Ther.* **1976**, *19*, 802-806.

(31) Obianom, O. N.; Ai, Y.; Li, Y.; Yang, W.; Guo, D.; Yang, H.; Sakamuru, S.; Xia, M.; Xue, F.; Shu, Y. Triazole-based inhibitors of the Wnt/β-catenin signaling pathway improve glucose and lipid metabolisms in diet-induced obese mice. *J. Med. Chem.* **2019**, *62*, 727-741.

(32) Hagland, H. R.; Berg, M.; Jolma, I. W.; Carlsen, A.; Soreide, K. Molecular pathways and cellular metabolism in colorectal cancer. *Dig. Surg.* **2013**, *30*, 12-25.

(33) Pelucchi, C.; Negri, E.; Talamini, R.; Levi, F.; Giacosa, A.; Crispo, A.; Bidoli, E.; Montella, M.; Franceschi, S.; La Vecchia, C. Metabolic syndrome is associated with colorectal cancer in men. *Eur. J. Cancer* **2010**, *46*, 1866-1872.

(34) Song, X.; Kim, S. Y.; Zhang, L.; Tang, D.; Bartlett, D. L.; Kwon, Y. T.; Lee, Y. J. Role of AMP-activated protein kinase in cross-talk between apoptosis and autophagy in human colon cancer. *Cell Death Dis.* **2014**, *30*, 463.

(35) Kim, I.; He, Y. Y. Targeting the AMP-activated protein kinase for cancer prevention and therapy. *Front. Oncol.* **2013**, *3*, 175.

(36) Zulato, E.; Bergamo, F.; De Paoli, A.; Griguolo, G.; Esposito, G.; De Salvo, G. L.; Mescoli, C.; Rugge, M.; Nardin, M.; Di Grazia, L.; Lonardi, S.; Indraccolo, S.; Zagonel, V. Prognostic significance of AMPK activation in advanced stage colorectal cancer treated with chemotherapy plus bevacizumab. *Br. J. Cancer* **2014**, *111*, 25-32.

(37) Din, F. V. N.; Valanciute, A.; Houde, V. P.; Zibrova, D.; Green, K. A.; Sakamoto, K.; Alessi, D. R.; Dunlop, M. G. Aspirin inhibits mTOR signaling, activates AMP-activated protein kinase, and induces autophagy in colorectal cancer cells. *Gastroenterology* **2012**, *142*, 1504-15.e3.

(38) Lea, M. A.; Pourat, J.; Patel, R.; desBordes, C. Growth inhibition of colon cancer cells by compounds affecting AMPK activity. *World J. Gastrointest. Oncol.* **2014**, *6*, 244-252.

(39) Zhao, Z.; Feng, L.; Wang, J.; Cheng, D.; Liu, M.; Ling, M.; Xu, W.; Sun, K. NPC-26 kills human colorectal cancer cells via activating AMPK signaling. *Oncotarget* **2017**, *8*, 18312-18321.

(40)Mogavero, A.; Maiorana, M. V.; Zanutto, S.; Varinelli, L.; Bozzi, F.; Belfiore, A.; Volpi, C. C.; Gloghini, A.; Pierotti, M. A.; Gariboldi, M. Metformin transiently inhibits colorectal cancer cell proliferation as a result of either AMPK activation or increased ROS production. *Sci. Rep.* **2017**, *7*, 15992-15992.

(41)Horn, T.; Ferretti, S.; Ebel, N.; Tam, A.; Ho, S.; Harbinski, F.; Farsidjani, A.; Zubrowski, M.; Sellers, W. R.; Schlegel, R.; Porter, D.; Morris, E.; Wuerthner, J.; Jeay, S.; Greshock, J.; Halilovic, E.; Garraway, L. A.; Caponigro, G.; Lehár, J. High-order drug combinations are required to effectively kill colorectal cancer cells. *Cancer Res.* **2016**, *76*, 6950-6963.

(42)Cheng, H.; Chang, Y.; Zhang, L.; Luo, J.; Tu, Z.; Lu, X.; Zhang, Q.; Lu, J.; Ren, X.; Ding, K. Identification and optimization of new dual inhibitors of B-Raf and epidermal growth factor receptor kinases for overcoming resistance against vemurafenib. *J. Med. Chem.* **2014**, *57*, 2692-2703.

(43)Zhang, Y. L.; Guo, H.; Zhang, C. S.; Lin, S. Y.; Yin, Z.; Peng, Y.; Luo, H.; Shi, Y.; Lian, G.; Zhang, C.; Li, M.; Ye, Z.; Ye, J.; Han, J.; Li, P.; Wu, J. W.; Lin, S. C. AMP as a low-energy charge signal autonomously initiates assembly of AXIN-AMPK-LKB1 complex for AMPK activation. *Cell Metab.* **2013**, *18*, 546-555.

(44)Obianom, O.; Yang, W.; Xue, F.; Shu, Y.: Tankyrases are druggable targets for the treatment of metabolic disorders. *FASEB J.* **2016**, *30*, 1189.5-1189.5.

(45)Hewitt, R. E.; McMarlin, A.; Kleiner, D.; Wersto, R.; Martin, P.; Tsoskas, M.; Stamp, G. W. H.; Stetler-Stevenson, W. G. Validation of a model of colon cancer progression. *J.*

Pathol. **2000**, *192*, 446-454.

(45) Zhou, G.; Myers, R.; Li, Y.; Chen, Y.; Shen, X.; Fenyk-Melody, J.; Wu, M.; Ventre, J.; Doebber, T.; Fujii, N.; Musi, N.; Hirshman, M. F.; Goodyear, L. J.; Moller, D. E. Role of AMP-activated protein kinase in mechanism of metformin action. *J. Clin. Invest.* **2001**, *108*, 1167-1174.

(46) Hawley, S. A.; Fullerton, M. D.; Ross, F. A.; Schertzer, J. D.; Chevtzoff, C.; Walker, K. J.; Peggie, M. W.; Zibrova, D.; Green, K. A.; Mustard, K. J.; Kemp, B. E.; Sakamoto, K.; Steinberg, G. R.; Hardie, D. G. The ancient drug salicylate directly activates AMP-activated protein kinase. *Science* **2012**, *336*, 918-922.

(47) Hewitt, R. E.; McMarlin, A.; Kleiner, D.; Wersto, R.; Martin, P.; Tsoskas, M.; Stamp, G. W. H.; Stetler-Stevenson, W. G. Validation of a model of colon cancer progressioin. *J. Pathol.* **2000**, *192*, 446-454.

(48) Cardia, M. C.; Corda, L.; Fadda, A. M.; Maccioni, A. M.; Maccioni, E.; Plumitallo, A. New cycloalkylpyrazoles as potential cyclooxygenase inhibitors. *Farmaco* **1998**, *53*, 698-708.

(49) Datterl, B.; Trostner, N.; Kucharski, D.; Holzer, W. Heterocyclic analogues of xanthone and xanthione. 1*H*-pyrano[2,3-c:6,5-c]dipyrazol-4(7*H*)-ones and thiones: synthesis and NMR data. *Molecules* **2010**, *15*, 6106-6126.

GRAPHIC ABSTRACT